

AD A 040 460

DYNAMICS AND FAILURE CRITERIA OF STRUCTURAL CONNECTIONS

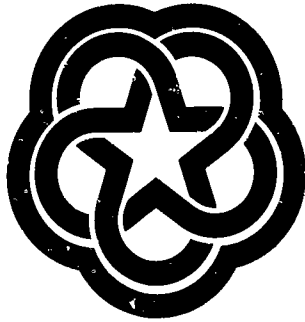
12

J. H. SMITH  
K. L. HOITSMA  
W. P. VANN

DEPARTMENT OF CIVIL ENGINEERING

FINAL REPORT

MAY 1977



*Sponsored by*

AIR FORCE OFFICE OF SCIENTIFIC RESEARCH  
AIR FORCE SYSTEMS COMMAND-USAF

*and*

AIR FORCE ARMAMENT LABORATORY  
VULNERABILITY ASSESSMENTS BRANCH  
AFSC, USAF, EGLIN AFB, FLORIDA

*Under*

GRANT NO. AFOSR-76-2976

DDC  
RECEIVED  
JUN 13 1977  
RECEIVED  
C

AD No. \_\_\_\_\_  
DDC FILE COPY

TEXAS TECH UNIVERSITY

Lubbock, Texas 79409

Qualified requestors may obtain additional copies from the Defense Documentation Center, all others should apply to the National Technical Information Service.

AIR FORCE OFFICE OF SCIENTIFIC RESEARCH (AFOSR)  
NOTICE OF TRANSMITTAL TO DDC  
This technical report has been reviewed and is  
approved for public release under AFOSR-12 (75).  
Distribution is unlimited.  
A. D. BLOSE  
Technical Information Officer

Conditions of Reproduction

Reproduction, translation, publication, use and disposal in whole or in part by or for the United States Government is permitted.

UNCLASSIFIED

SECURITY CLASSIFICATION OF THIS PAGE (When Data Entered)

REPORT DOCUMENTATION PAGE		READ INSTRUCTIONS BEFORE COMPLETING FORM
1. REPORT NUMBER (A) AFOSR TR-77-030, UR-77-12	2. GOVT ACCESSION NO.	3. RECIPIENT'S CATALOG NUMBER
(A) AFAPL		4. TYPE OF REPORT & PERIOD COVERED (9) FINAL REP 1 Feb 76 - 31 Jan 77
(6) DYNAMICS AND FAILURE CRITERIA OF STRUCTURAL CONNECTIONS		5. PERFORMING ORG. REPORT NUMBER
7. AUTHOR(s) J. H. Smith, K. L. Hoitsma W. P. Nann		8. CONTRACT OR GRANT NUMBER(s) 15/AF-AFOSR 85-2976-76
9. PERFORMING ORGANIZATION NAME AND ADDRESS Texas Tech University Department of Civil Engineering Lubbock, Texas 79409		10. PROGRAM ELEMENT, PROJECT, TASK AREA & WORK UNIT NUMBERS (10) 9782-04 17 C.F. 61102F
11. CONTROLLING OFFICE NAME AND ADDRESS Air Force Office of Scientific Research Building 410 Bolling Air Force Base, D.C. 20332		12. REPORT DATE (11) May 1977
14. MONITORING AGENCY NAME & ADDRESS (if different from Controlling Office)		13. NUMBER OF PAGES 12-977
		15. SECURITY CLASS. (of this Report)  UNCLASSIFIED
		15a. DECLASSIFICATION/DOWNGRADING SCHEDULE
16. DISTRIBUTION STATEMENT (of this Report)  Approved for public release; distribution unlimited.		
17. DISTRIBUTION STATEMENT (of the abstract entered in Block 20, if different from Report)  D D C RESTRICTED RESTRICTED C		
18. SUPPLEMENTARY NOTES		
19. KEY WORDS (Continue on reverse side if necessary and identify by block number) STRUCTURES CONCRETE DYNAMICS BURIED ARCHES CONNECTIONS HIGH STRAIN RATES		
20. ABSTRACT (Continue on reverse side if necessary and identify by block number) This research was conducted to establish new knowledge of failure criteria for concrete connections which will enable the USAF to predict, with acceptable accuracy, the failure modes of aircraft shelters. Of primary importance was the effect of extremely high stress rates on ultimate failure strength of the crown connections. A total of seven static and fourteen dynamic tests were conducted and comparison made of the two test series to establish a dynamic strength factor. A drop-tower was constructed for the dynamic tests which		

~~UNCLASSIFIED~~

SECURITY CLASSIFICATION OF THIS PAGE (When Data Entered)

enabled rise times to failure of under 4 milliseconds to be achieved. Although most of the effort was concentrated on full-scale connections, static tests to failure were also conducted on one-third scale models. These results, when considering the effects of scaling, were in agreement with full-scale tests. For the complicated loading of bending and tension on a connection, the resulting dynamic strength factor was determined to be 1.3, or 130 percent of static tensile strength.

UNCLASSIFIED

DYNAMICS AND FAILURE CRITERIA OF STRUCTURAL CONNECTIONS

by

J. H. Smith, Principal Investigator  
K. L. Hoitsma, Research Assistant  
W. P. Vann, Investigator

DEPARTMENT OF CIVIL ENGINEERING  
TEXAS TECH UNIVERSITY  
LUBBOCK, TEXAS 79409

Final Report on Grant No.  
AFOSR 76-2976 from the Air Force  
Office of Scientific Research

May 1977

✓

A

## FOREWORD

The research was sponsored by the Air Force Office of Scientific Research, Air Force Systems Command, USAF, under Grant No. AFOSR-76-2976. Funds were provided by the Air Force Armament Laboratory, Armament Development and Test Center (ADTC), Eglin Air Force Base, Florida under Obligation Authorities 76-Y-13. Mr. Phillip T. Nash (DLYV) was the technical program manager for the Armament Laboratory.

The effort was begun on 1 February 1976 and was completed on 31 January 1977.

The United States Government is authorized to reproduce and distribute reprints for Governmental purposes notwithstanding any copyright notation hereon.

A supplement to this grant involved an initial study of dynamics of a horizontal stabilator. Subsequent funding of a much more detailed research project specifically involving stabilators was granted under AFOSR Grant No. 77-3231 and, therefore, results of research on stabilators will be reported in the technical report of that project.

## ABSTRACT

### DYNAMICS AND FAILURE CRITERIA OF STRUCTURAL CONNECTIONS

This research was conducted to establish new knowledge of failure criteria for concrete connections which will enable the USAF to predict, with acceptable accuracy, the failure modes of aircraft shelters. Of primary importance was the effect of extremely high stress rates on ultimate failure strength of the crown connections. A total of seven static and fourteen dynamic tests were conducted and comparison made of the two test series to establish a dynamic strength factor. A drop-tower was constructed for the dynamic tests which enabled rise times to failure of under 4 milliseconds to be achieved. Although most of the effort was concentrated on full-scale connections, static tests to failure were also conducted on one-third scale models. These results, when considering the effects of scaling, were in agreement with full-scale tests. For the complicated loading of bending and tension on a connection, the resulting dynamic strength factor was determined to be 1.3, or 130 percent of static tensile strength.

## TABLE OF CONTENTS

	Page
LIST OF TABLES .....	v
LIST OF FIGURES .....	vi
I. INTRODUCTION .....	1
II. PAST RESEARCH .....	3
III. TEST SPECIMENS .....	6
A. Concrete Arch .....	6
B. Concrete Connection Specimens .....	6
C. Concrete Cylinder Specimens .....	17
IV. DESCRIPTION OF EXPERIMENTAL EQUIPMENT .....	19
A. Forney Testing Machine .....	19
B. Hydraulic Rams .....	19
C. Vishay/Ellis Strain Measurement System .....	19
D. Tektronix Type Q Plug-In Unit .....	19
E. Tektronix Oscilloscope .....	23
F. Tektronix Camera System .....	23
G. Tinius-Olsen UEH Testing Machine .....	25
H. Strain Gages .....	25
I. Hycam Movie Camera .....	25
V. EXPERIMENTAL PROCEDURES .....	28
A. Introduction .....	28
B. Static Testing of Connections .....	28
C. Dynamic Testing of Connections .....	31
D. Static Concrete Cylinder Tests .....	34

	<u>Page</u>
VI. EXPERIMENTAL RESULTS .....	38
A. Static Connection Tests .....	38
B. Dynamic Connection Tests .....	45
C. Static Cylinder Test Results .....	68
D. Reinforcing Bar Tests .....	68
VII. SUMMARY, CONCLUSIONS, AND RECOMMENDATIONS .....	72
BIBLIOGRAPHY .....	75
APPENDIX A. ONE-THIRD SCALE ARCH SPECIMENS .....	78
APPENDIX B. CALCULATIONS .....	80

LIST OF TABLES

<u>Tables</u>	<u>Page</u>
1. Connection Casting Schedule .....	18
2. Static Connection Test Results .....	39
3. Dynamic Connection Test Results .....	46
4. Individual Static Concrete Cylinder Tests (Compression and Splitting) .....	66
5. Batch Cylinder Test Results .....	67
6. Reinforcing Bar Test Results .....	71
7. Theoretical vs. Experimental Cracking Loads (Static Tests) .....	84

## LIST OF FIGURES

	<u>Page</u>
II-1. Stress Rate vs. Dynamic Strength Factor .....	4
III-1. Prototype Reinforced Concrete Barrel Arch .....	7
III-2. Individual Rib Specifications .....	8
III-3. Typical Arch Rib Member .....	9
III-4A. Connection for Static Test .....	10
III-4B. Connection for Dynamic Test .....	11
III-4C. Reinforcement of Dynamic Test Connection .....	12
III-4D. Reinforcement of Dynamic Test Connection .....	13
III-4E. Reinforcement of Dynamic Test Connection .....	14
III-4F. Reinforcement of Static Test Connection (Front and Side View) .....	15
III-5A. Static Test Connection .....	16
III-5B. Dynamic Test Connection .....	16
IV-1. Forney Testing Machine .....	20
IV-2. Hydraulic Pump and Rams .....	21
IV-3. Vishay/Ellis Strain Measurement System .....	22
IV-4. Tektronix Type Q Plug-In Unit .....	22
IV-5. Tektronix 545 Oscilloscope and Camera System .....	24
IV-6. Tinius-Olsen UEH Testing Machine .....	26
IV-7. Strain-Gaged Bolt .....	27
IV-8. Hycam Motion Picture Camera .....	27
V-1. Laboratory Layout for Static Test .....	29
V-2. Component Identification: Static Tests .....	30
V-3. Dynamic Connection Test Frame .....	33
V-4. Standard Concrete Cylinder Tests .....	35

	<u>Page</u>
V-5. Split Cylinder Test .....	37
VI-1A. Static Connection One .....	40
VI-1B. Static Connection Two .....	40
VI-1C. Static Connection Three .....	41
VI-1D. Static Connection Four .....	41
VI-1E. Static Connection Five .....	42
VI-1F. Static Connection Six .....	42
VI-2A. Load Vs. Crack Width for Static Test No. 5 ... ..	44
VI-2B. Load Vs. Crack Width for Static Test No. 6 .....	45
VI-3A. Dynamic Connection One .....	47
VI-3B. Dynamic Connection Two .....	48
VI-3C. Dynamic Connection Three .....	49
VI-3D. Dynamic Connection Four .....	50
VI-3E. Dynamic Connection Five .....	51
VI-3F. Dynamic Connection Six .....	52
VI-3G. Dynamic Connection Seven .....	53
VI-3H. Dynamic Connection Eight .....	54
VI-3I. Dynamic Connection Nine .....	55
VI-3J. Dynamic Connection Ten .....	56
VI-3K. Dynamic Connection Eleven .....	57
VI-3L. Dynamic Connection Twelve .....	58
VI-3M. Dynamic Connection Thirteen .....	59
VI-4. Typical Dynamic Test Record .....	60
VI-5A. Dynamic Test No. 5 .....	61
VI-5B. Dynamic Test No. 7 ... ..	61

	<u>Page</u>
VI-5C. Dynamic Test No. 8 .....	62
VI-5D. Dynamic Test No. 9 .....	62
VI-5E. Dynamic Test No. 11 .....	63
VI-5F. Dynamic Test No. 12 .....	63
VI-5G. Dynamic Test No. 13 .....	64
VI-5H. Dynamic Test No. 14 .....	64
VI-6. Superposed Dynamic Test Records .....	65
VI-7. Reinforcing Bar Tests .....	69

## I. INTRODUCTION

Model concrete arches have been studied for the last two years at Texas Tech under funding from the Air Force Office of Scientific Research (AFOSR). This funding has come through a grant entitled "Theoretical and Experimental Investigation of Buried Concrete Structures" (Grant Number AFOSR 76-2976). In this program, one-third scale reinforced concrete arch models constructed by the Air Force have been used by Texas Tech to determine fundamental modes for two types of conditions: (1) the bare arch and (2) the soil-covered arch. The full-scale structure has been field tested previously to determine its fundamental frequencies. Full- and one-third scale test results have been used to verify the accuracy of computer code predictions of the structural responses of buried concrete arches.

Once verification of the computer program's ability to predict steady state and free vibration was documented, internal blast loads were simulated in the computer and printouts of the "arch response" were studied. In these studies, the researchers were faced with the difficulty of incorporating into the computer code the dynamic material properties of concrete, particularly at connections. Previous research has been conducted which identifies both the dynamic compressive stress-strain properties and the dynamic compressive failure stresses of plain concrete. Insufficient research had been accomplished, however, on the dynamic tensile properties of plain concrete to ensure the proper simulation of concrete behavior under blast conditions. For instance, in the concrete research literature, the fastest stress rates for tensile loads were approximately 300 ksi per second [7], whereas, estimates of stress rates for the internal blast problem ranged as high as 400 ksi per second. Thus the need for basic knowledge for these higher tensile stress rates and their effect on concrete was apparent.

The scope of the research included static and dynamic testing of concrete cylinder and structural connections. The dynamic test specimens were to be tested at stress rates sufficient to cause a tension failure of the concrete within a range of five to thirty milliseconds in both the cylinders and the connections. Thus, two drop tower facili-

ties needed to be designed and constructed to accommodate the dynamic tests of both cylinders and connections. Several attempts were made to construct a satisfactory drop tower for cylinder testing; this effort was not successful and no dynamic test results for cylinders are included in this report. For dynamic testing of connections, however, the drop tower developed was of a somewhat unorthodox design in that instead of using a stationary specimen and moving loading device, the specimen itself was dropped and "caught", thereby loading itself to failure by virtue of its own inertia.

The static connection specimens were to be tested to failure under gradually applied tensile loads. A custom-designed test frame was constructed in the laboratory for this purpose. Manually controlled hydraulic rams were utilized in the testing of these static connections.

Of the 24 connections cast, 21 were tested--7 statically and 14 dynamically. A total of 120 cylinders were made of which 36 were tested statically; no dynamic tests were made on cylinders.

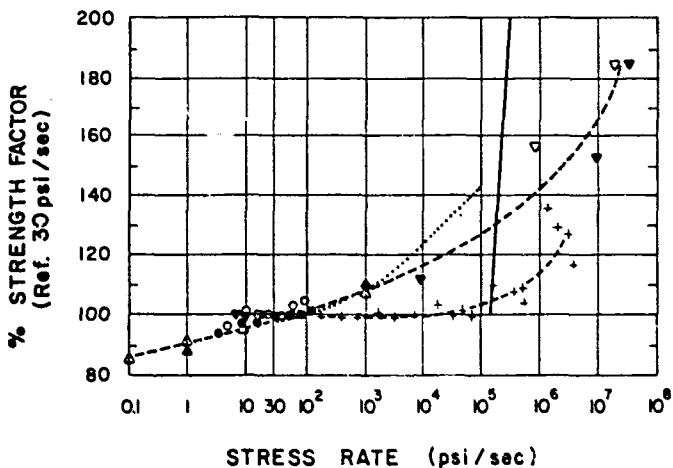
## II. PAST RESEARCH

In 1917, Abrams conducted the first reported dynamic tests on concrete [1]. His conclusions were simply that the strength of concrete increased with an increase in the rate of loading. Jones and Richart concluded from tests completed in 1936 that an increase in compressive strength was associated with an increase in the rate of loading [13]. Presented in Figure II-1 are the published results of experiments performed by several investigators in which the strain (or stress) rate sensitivity of concrete was measured. In this figure only the results of Keenan and Crist are from investigation of tensile strain-rate sensitivity.

Dynamic and static compressive tests were performed by Watstein in 1953 from which he concluded that as the rate of loading increases: (1) compressive strength increases, (2) the modulus of elasticity increases, (3) the strain energy absorbed increases, and (4) the total strain at failure increases [26]. Impact experiments were done in 1966 by Cowell which showed that the energy absorption capacity of concrete is higher if the concrete is subjected to higher load rates [6].

Atchley and Furr have concluded as a result of experiments completed in 1967 that an increase in load rate will increase the secant modulus and the total strain at failure [3]. Also, their report indicates that compressive strength and energy absorbed increase with loading rate although evidence of levelling off was present at higher rates of loading.

Keenan published a report in 1976 [14] in which studies of dynamic tensile strengths of concrete were discussed. This report indicated an increase in the tensile strength of concrete accompanying an increase in the stress rate. In 1967, Crist [7] concluded as a result of tests on tensile strain-rate sensitivity that concrete has a higher tensile strength when subjected to higher load rates. Both Keenan and Crist used the standard split-cylinder test in determining tensile strength.



LEGEND :

○	BUREAU OF RECLAMATION	8" x 16" CYLINDERS
●	BUREAU OF RECLAMATION	6" x 12" CYLINDERS
△	JONES & RICHART	6" x 12" CYLINDERS - 7 DAYS
▲	JONES & RICHART	6" x 12" CYLINDERS - 28 DAYS
▽	WATSTEIN	3" x 6" CYLINDERS - "WEAK"
▼	WATSTEIN	3" x 6" CYLINDERS - "STRONG"
■	ASTM COMMITTEE C-1	2" CUBES
+	EVANS	2" & 3" CUBES
—	CRIST (TENSION)	6" x 6" CYLINDERS
.....	KEENAN (TENSION)	CYLINDERS

FIGURE II-1. STRESS RATE VS DYNAMIC STRENGTH FACTOR

Research was performed by Mavis and Graves in 1957 on the destructive impulse loading of concrete beams. Although the research was conducted to study steel reinforcement response to dynamic loads at least one pertinent observation was made by the authors concerning the dynamic strength of concrete. The maximum dynamic strength factor of the concrete beams was approximately 2.1.

Of course, there is no standard dynamic strength tests for either plain or reinforced concrete. Each investigator of the dynamic properties of concrete has had certain objectives to be met and accordingly applied his ingenuity in devising such tests as were necessary. Primarily, past tests have relied on the compression test to determine the strain-rate dependent characteristics of plain concrete. The compression specimen sizes and shapes have varied from project to project, yet the overall compression results shown in Figure II-1 seem to follow the same general pattern.

Split-cylinder tests were utilized by Keenan and Crist in determining the dynamic strength factor with respect to load rate. Their results differ in at least one major respect: Keenan shows the dynamic strength factor as being approximately 130 percent at a load rate of 150,000 psi per second but, according to Crist, a value of 100 percent should be used. Logically, the 100 percent value should only occur, for a strain-rate dependent material, at a stress-rate of 300 psi per second, the reference loading rate. The gradual increase in the strength factor predicted by Keenan's plotted curve appears more logical in this respect.

### III. TEST SPECIMENS

#### A. Concrete Arch

For completeness and understanding, a description of the entire prototype structure is presented. The semicircular barrel arch shown in Figure III-1 is made up of prefabricated concrete ribs. Twenty reinforced ribs, each having a width of  $39 \frac{3}{8}$  inches, are assembled side by side to form the complete arch. The inside radius of the arch is 17 feet 6 inches and its length is 65 feet  $7 \frac{1}{2}$  inches. Individual rib specifications are presented in Figure III-2. A typical semicircular rib (See Figure III-3) is made up to two prefabricated quarter-circle elements which are bolted together at the crown with two one-inch diameter steel bolts. The arch is supported on a keyway on either side at ground level.

Since the tensile behavior of the crown regions was of immediate interest, test specimens were chosen which modeled only the crown vicinity of the quarter-circle elements.

#### B. Concrete Connection Specimens

Beams with relatively large radii of curvature with respect to their thickness behave very much like straight beams [22]. Because of this behavior and because of the desire to simplify casting operations, the connection specimens were cast as straight beams. Preliminary calculations indicated the dynamic specimen needed to weigh at least 1000 pounds to produce the necessary inertia forces. Finally, because of forming considerations, a length of 47 inches was used in casting the specimens. This length resulted in an average weight per specimen of approximately 1450 pounds.

Two types of specimens were constructed: static and dynamic. Figure III-4 details the dimensions and reinforcing placement for these connections. Photographs of each type of specimen are shown in Figure III-5. The slightly heavier static connections were equipped with two diaphragms: one,  $4 \frac{1}{2}$  inches thick which was to be tested;

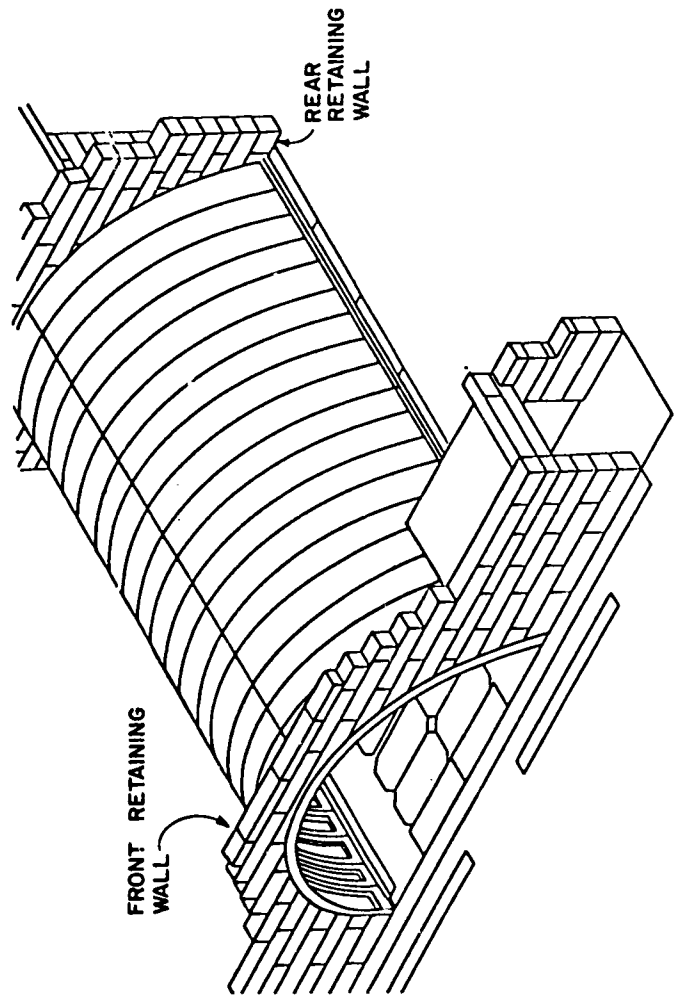


FIGURE I.1.1-1. PROTOTYPE REINFORCED CONCRETE BARREL ARCH

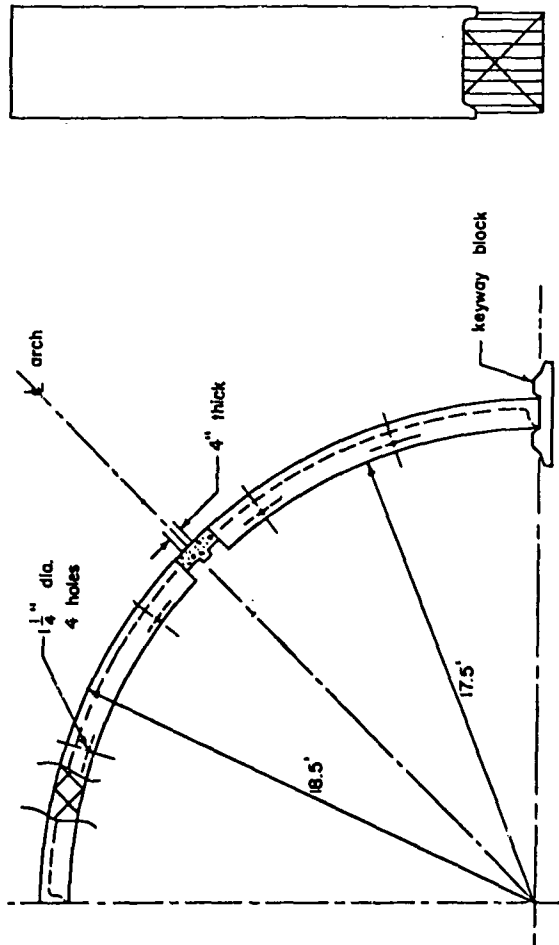


FIGURE III-2. INDIVIDUAL RIB SPECIFICATIONS

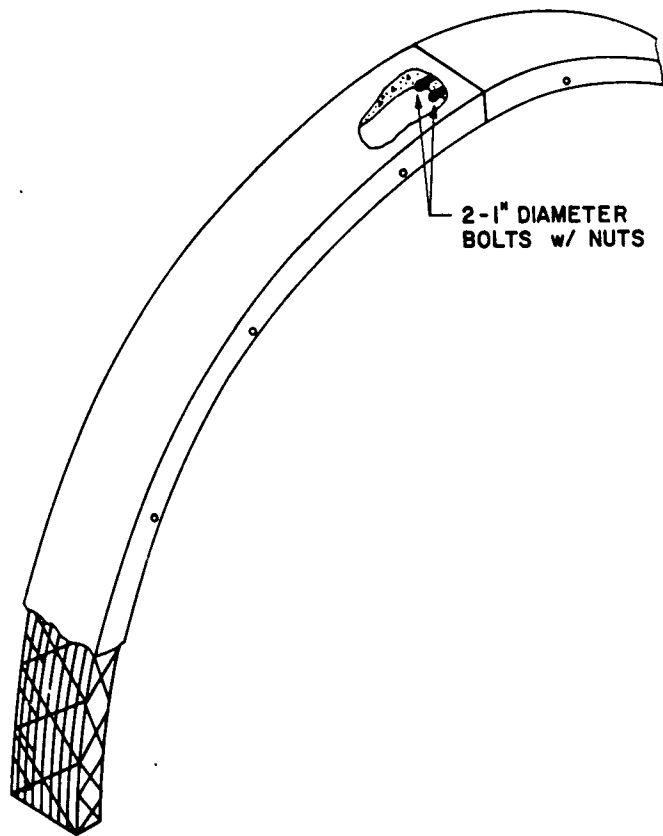


FIGURE III-3. TYPICAL ARCH RIB MEMBER

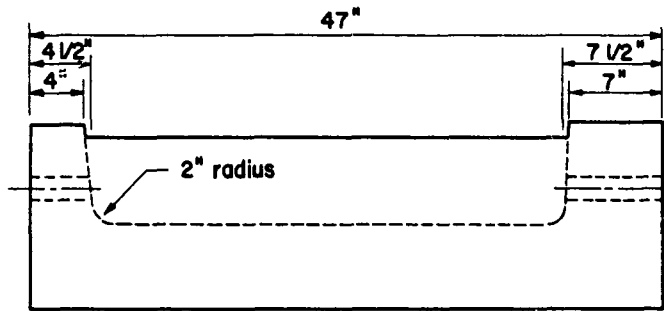
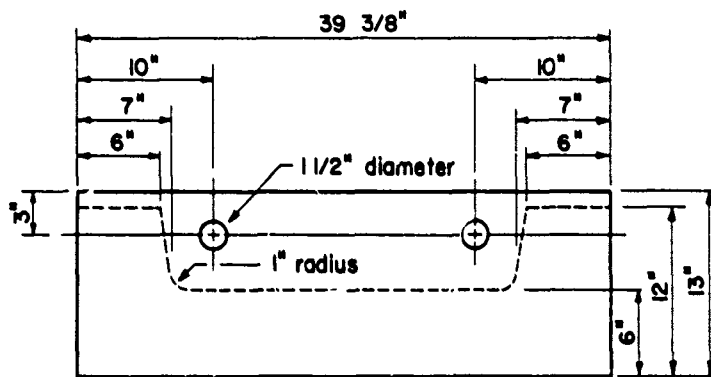
SIDE VIEWEND VIEW

FIGURE III-4A. CONNECTION FOR STATIC TEST

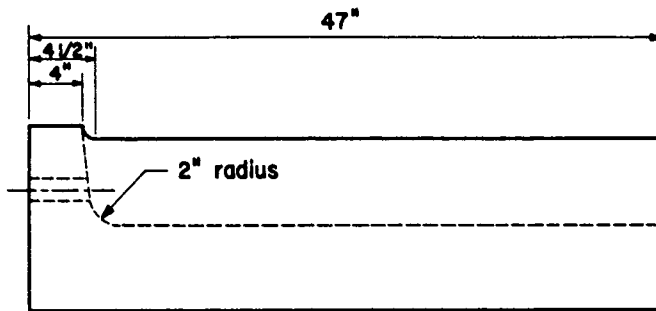
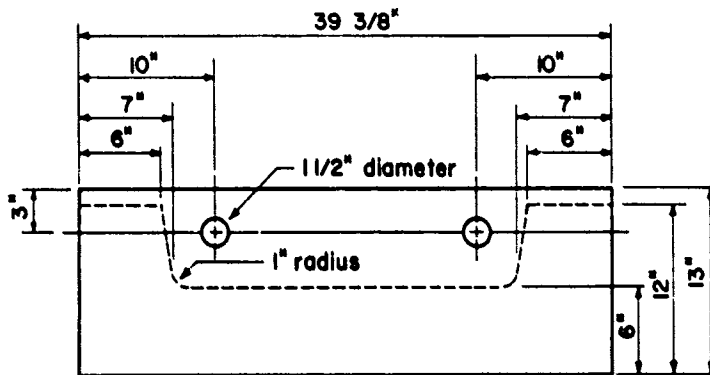
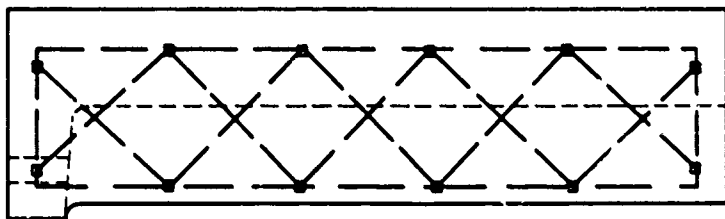
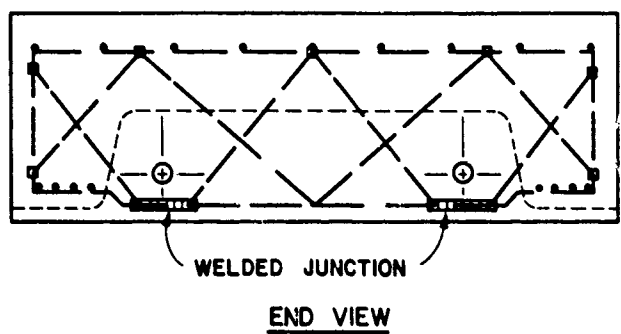
SIDE VIEWEND VIEW

FIGURE III-4B. CONNECTION FOR DYNAMIC TESTS

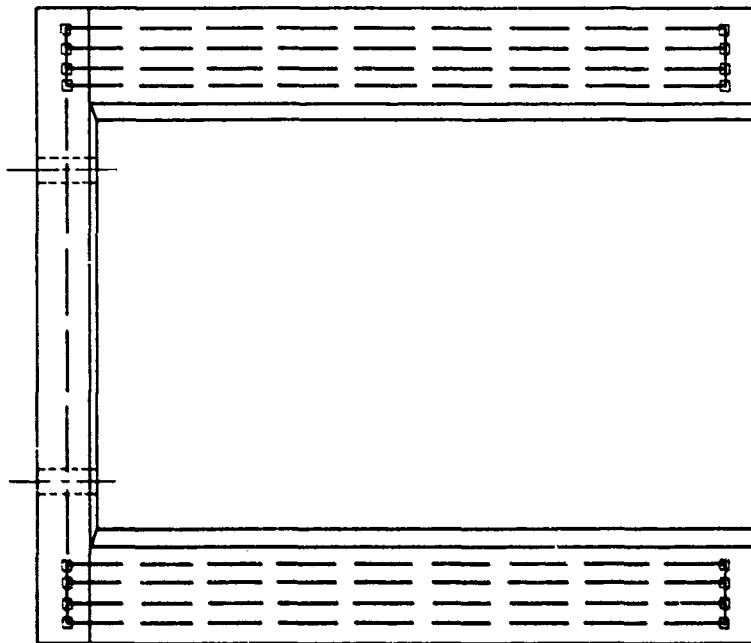


□ - DENOTES WELDED JUNCTION

scale: 1 1/2" = 1' - 0"

SIDE VIEW

FIGURE III-4C. REINFORCEMENT OF DYNAMIC TEST CONNECTION

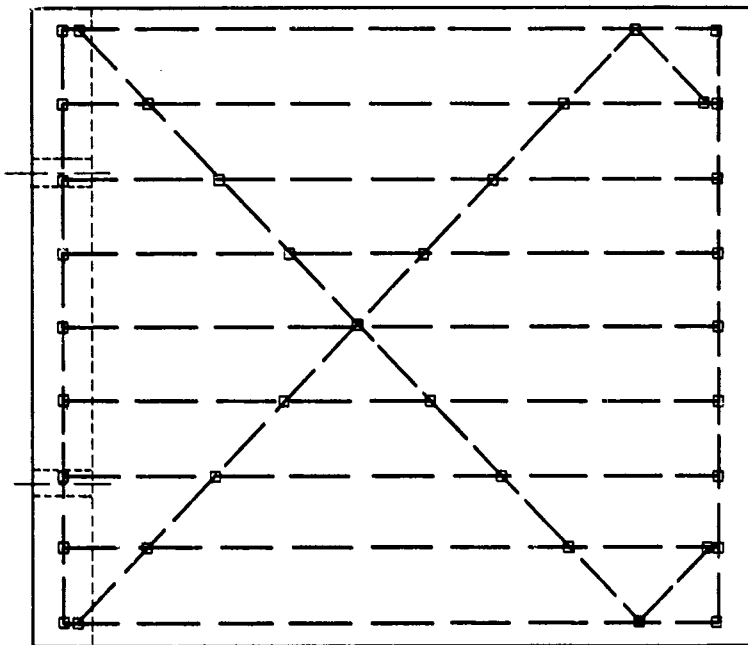


□ - DENOTES WELDED JUNCTION

scale:  $1\frac{1}{2}'' = 1'-0''$

BOTTOM VIEW

FIGURE III-4D. REINFORCEMENT OF DYNAMIC TEST CONNECTION



□ - DENOTES WELDED JUNCTION

scale :  $1\frac{1}{2}'' = 1'-0''$

TOP VIEW

FIGURE III-4E. REINFORCEMENT OF DYNAMIC TEST CONNECTION

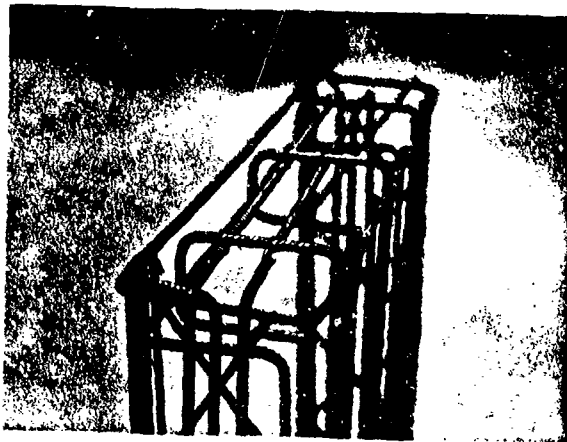
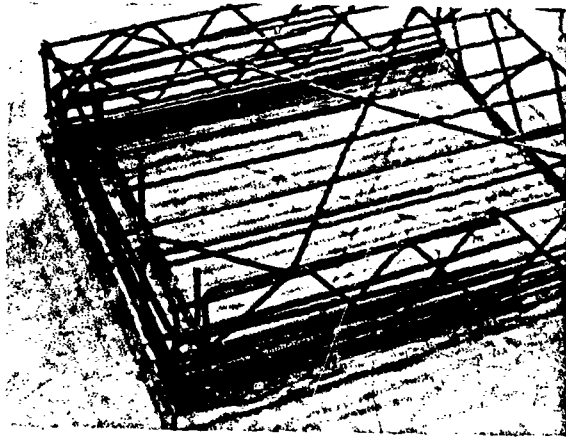


FIGURE III-4F. REINFORCEMENT OF STATIC TEST CONNECTION  
(FRONT AND SIDE VIEW)



FIGURE III-5B. DYNAMIC TEST CONNECTION

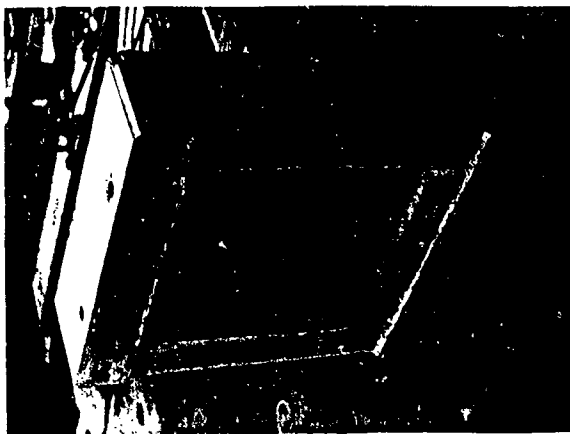


FIGURE III-5A. STATIC TEST CONNECTION

and another 7 inches thick, used to provide a means of applying load. The dynamic connection was fabricated with only one diaphragm. Since inertia loads were to be used in the dynamic testing of connections, the second diaphragm was unnecessary.

Table 1 presents the details of the construction of all 24 connections. Within the 24 specimens there are two types of steel reinforcement:

- (1) Deformed, #3, Grade 60 steel reinforcement and
- (2) Smooth, 65 ksi, M1020 round steel bar, 7/16 inch and 3/8 inch diameter.

Further, two techniques of constructing reinforcing cages were employed. In all of the connections cast on 5/11/76, cages were constructed of #3 rebar, wired at most junctions and "tack-welded" at all junctions where wiring could not be used due to geometry. However, in connections cast on all other dates, reinforcement cages were assembled as a single unit using welds only; the welding electrodes used were E6013. On 6/30/76, four connections were made using the smooth steel bar as reinforcement. From Batch #1, one static and one dynamic connection were made using 7/16 inch diameter steel while from Batch #2 a single static and a single dynamic connection were cast using 3/8 inch diameter steel as reinforcement. All specimens were cast by Crowe-Gulde, Inc. of Lubbock, Texas

### C. Concrete Cylinder Specimens

All concrete test cylinders were made according to ASTM C192-69. The single-use wax molds used conformed to ASTM C470-73T and were manufactured by Soiltest, Inc. In all, 120 cylinders were made, 20 cylinders on each of six separate casting dates. On each date, two batches of concrete were made; ten cylinders were cast from each batch. The large 5/8 inch diameter ASTM rod was used for tamping. All moist-curing was done in a moist cabinet which met specifications of ASTM C511-73. A slump test according to ASTM C143-71 was made on this initial casting date; it was 3/4-inch. Since the same mix was used throughout subsequent castings, additional slump tests were not made.

<u>Date Cast</u>	<u>Specimen Type and Number</u>	<u>Reinforcing Type</u>	<u>Reinforcing Cage Construction</u>
5/11/76	4 Dynamic	#3, Grade 60	Cages tied with wire, some junctions tack-welded
6/28/76	2 Dynamic 2 Static	#3, Grade 60	Cages welded
6/29/76	2 Dynamic 2 Static	#3, Grade 60	Cages welded
6/30/76	1 Dynamic 1 Static	Smooth, M1020, 65 ksi, 7/16" dia. steel bar	Cages welded
6/30/76	1 Dynamic 1 Static	Smooth, M1020, 65 ksi, 3/8" dia. steel bar	Cages welded
7/13/76	2 Dynamic 2 Static	#3, Grade 60	Cages welded
7/15/76	2 Dynamic 2 Static	#3, Grade 60	Cages welded

TABLE 1. CONNECTION CASTING SCHEDULE

#### IV. DESCRIPTION OF LABORATORY EQUIPMENT

##### A. Forney Testing Machine

All static concrete cylinder tests were performed using a 400,000 pound capacity Model QC 225 Forney Testing Machine. This machine is equipped with load rate settings corresponding to ASTM standards for concrete cylinder tests. Figure IV-1 illustrates a typical test setup for compression tests.

##### B. Hydraulic Rams

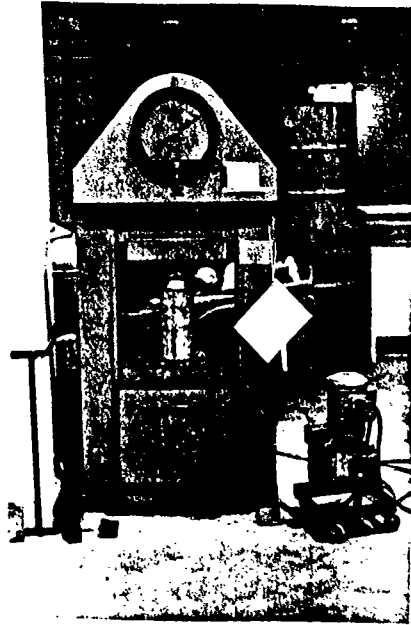
In the static testing of concrete connection specimens, six double-acting hydraulic rams were utilized. Each ram had an effective area in tension of 9.43 sq in. and a pressure rating of 2500 psi; therefore, the total tensile load capacity of the six rams was 141,000 pounds. These rams are shown in Figure IV-2.

##### C. Vishay/Ellis Strain Measurement System

A Vishay/Ellis-20A Digital Strain Indicator coupled with a V/E-21 switch, balance, and calibration unit was used to monitor total loads in the static tests in which strain-gage load cells were employed. This Vishay/Ellis System (See Figure IV-3) provided the capability of reading from zero to 1999 microstrains with a resolution of one microstrain. This equipment and the associated load-cell circuit was calibrated with the Tinius-Olsen UEH Testing Machine prior to the testing of each specimen.

##### D. Tektronix Type Q Plug-In Unit

A critical data-recording instrument used in this research was the Tektronix Type Q Transducer and Strain Gage Unit shown in Figure IV-4. This preamp unit was plugged into the Tektronix 545 Oscilloscope; the strain gage bridge circuit was attached to the Type Q Unit via external arms. The two-arm bridge was found to be satisfactory



FIGUP IV-1. FORNEY TESTING MACHINE

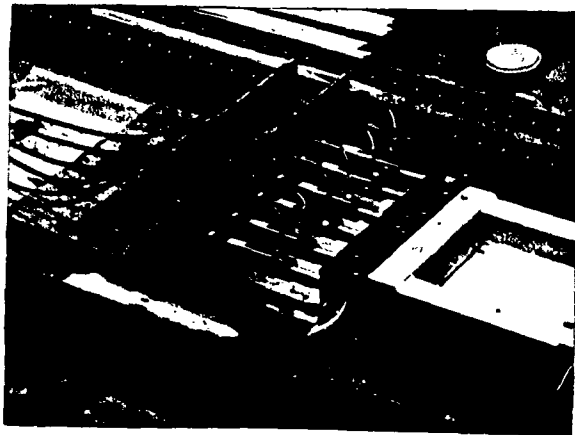
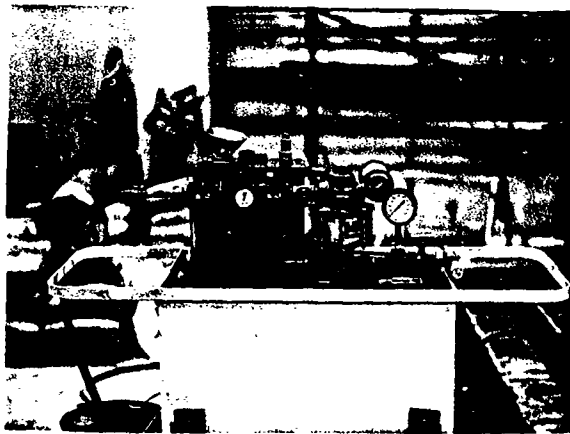


FIGURE IV-2. HYDRAULIC PUMP AND RAMS

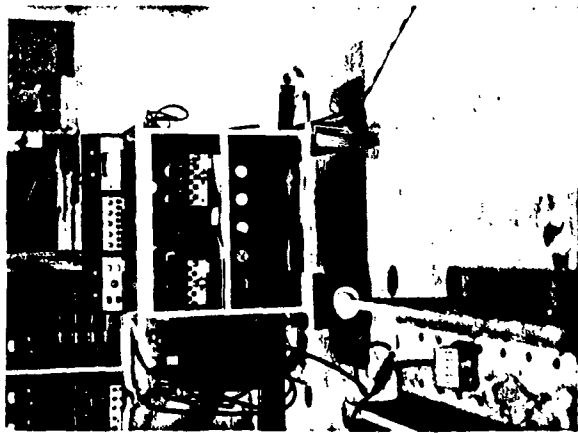


FIGURE IV-3. VISHAY/ELLIS STRAIN MEASUREMENT SYSTEM

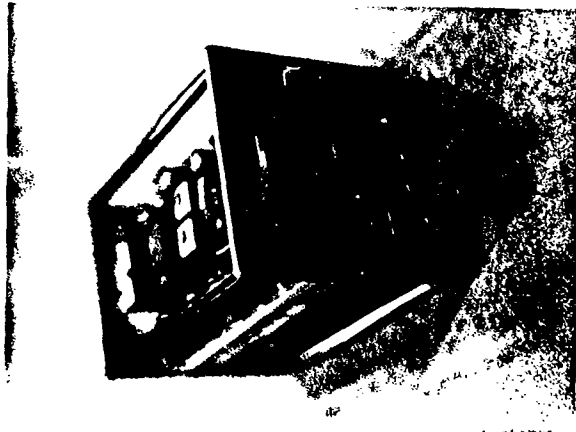


FIGURE IV-4. TEKTRONIX TYPE Q PLUG-IN UNIT

during calibration and actual testing conditions. Because of the lead lengths used (10 feet), the gage factor was found to decrease somewhat due to lead resistance. An experimental calibration technique was therefore devised whereby the two connection bolts could be simultaneously stressed under a known tensile load. The gain adjust of the strain gage unit was set such that the microstrain reading of the unit would correspond to the average strain level in the bolts. For this calibration the Timius-Olsen UEH Testing Machine was used for both loading and load measurement.

#### E. Tektronix Oscilloscope

The oscilloscope used in conjunction with the Type Q Transducer and Strain Gage Unit was a calibrated Model 545 Tektronix Oscilloscope (See Figure IV-5). This unit was equipped with an internal triggering mechanism capable of responding to positively or negatively sloped inputs. This trigger was used to produce a trace on the oscilloscope screen upon input of dynamic strains from the connection gages. A Tektronix Oscilloscope Camera System was mounted on the screen to preserve each trace on film. The rise-time of the vertical amplifier in the oscilloscope was measured as 0.01 microseconds. The range of oscilloscope sweep rate settings was from 0.1 to 2.0 milliseconds/centimeter.

#### F. Tektronix Camera System

The Tektronix Camera System (See Figure IV-5) consisted of a special oscilloscope and a Polaroid Land Camera Film Pack with mounting equipment. This system allowed the researcher to select shutter speeds and F-stops so as to provide an instantaneous hard copy of the oscilloscope trace. In this research the oscilloscope camera shutter speed was always set on "B", a shutter setting which allowed manual opening and closing of the shutter. An F-stop of 4 was found to be satisfactory for the sweep rates of 0.1 to 2 milliseconds/centimeter. Type 42 Polaroid Roll Film was used in all photographs.

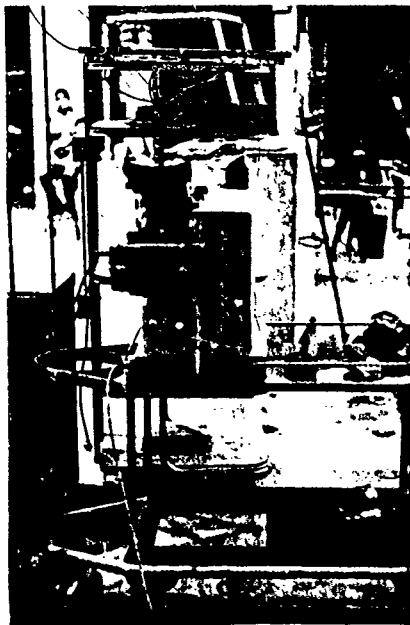


FIGURE IV-5. TEKTRONIX 545 OSCILLOSCOPE  
AND CAMERA SYSTEM

#### G. Tinius-Olsen UEH Testing Machine

All calibraton tests on load cells were performed using the UEH Testing Machine in the structural test laboratory at Texas Tech University. This machine is a servo-controlled 200,000 pound capacity hydraulic testing machine. The UEH may be operated in either load or position control and during loading both load and platen position may be electronically monitored. The operator's console and the loading platens of the Tinius-Olsen are shown in Figure IV-6.

#### H. Strain Gages

To measure failure loads in all tests, strain gages were mounted on a pair of 1-inch diameter bolts (Figure IV-7). In all experiments requiring strain measurement, Micro-Measurement EA06-250BG-120 strain gages were used. The gage length was 0.250 inches, the resistance was 120 ohms, and the gage factor was 2.095. Lead lengths for each strain gauge were approximately 10 feet. The lead resistance lowered the gage factor by a small percentage; however, before use of a strain-gaged load cell, a calibration check was made on the load readings. The loads as derived from the strains were calibrated to concur with the loads as measured by the Tinius-Olsen UEH Testing Machine. This calibration procedure eliminated the need for theoretical lead resistance corrections.

#### I. Hycam Movie Camera

The Hycam Camera used a high-speed 16 millimeter, 400 foot capacity, rotating prism movie camera (See Figure IV-8) loaned to Dr. J. H. Smith by Eglin Air Force Base, Florida. This particular camera, Model K2004E, is capable of a maximum of 11,000 pictures per second; however, in all tests at Texas Tech the exposure rate was only 1000 pictures per second. The dimness of the light prevented good movies of the dynamic tests from being developed.

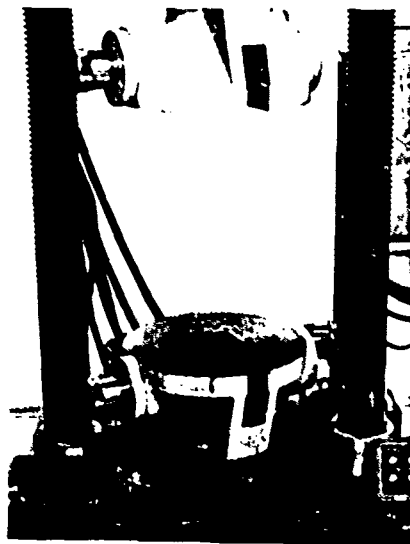
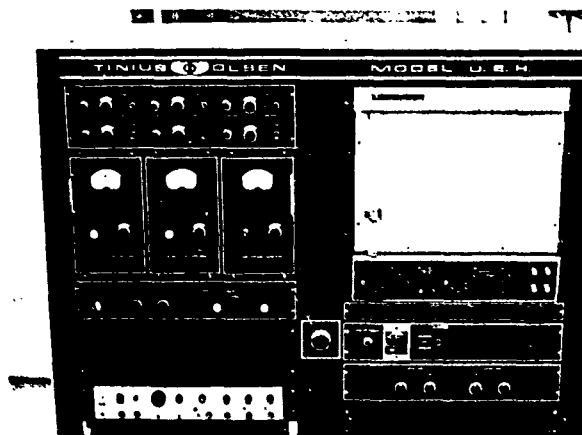


FIGURE IV-6. TINIUS-OLSEN UEH TESTING MACHINE

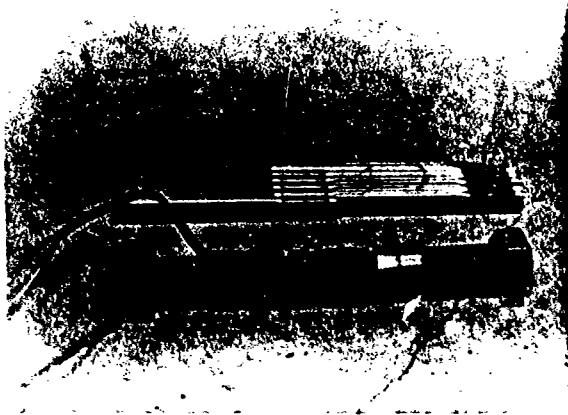


FIGURE IV-7. STRAIN-GAGED BOLT

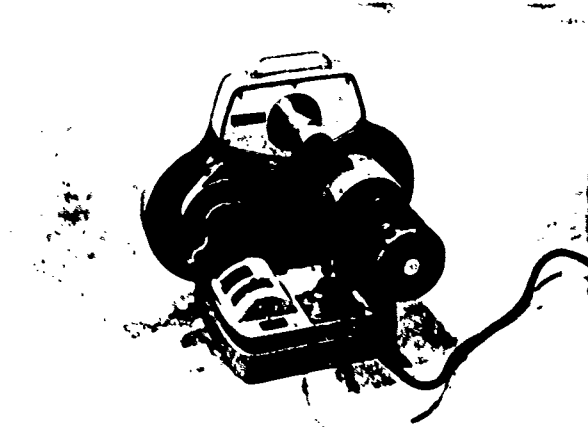


FIGURE IV-8. HYCAM MOTION PICTURE CAMERA

## V. EXPERIMENTAL PROCEDURES

### A. Introduction

This chapter will present the documentation of the five major laboratory test procedures used in the arch connection research. The first two procedures mentioned are the actual static and dynamic failure tests used on the connection specimens. The third procedure, and one of great importance, is the load-cell calibration procedure. Finally, the method of testing the steel and concrete material properties is described.

### B. Static Testing of Connections

Ten concrete connections were specially designed and constructed to be used in static tension tests. Three of these ten were used later as dynamic specimens. A description of construction details has been presented in Chapter III. In the static test phase of this connection research, the ultimate and failure load values were of most importance; however, identification of the modes of failure was considered to be crucial to understanding the concrete behavior. Accordingly, crack measurements were used to supplement the photographic records made of each static test.

A horizontal test setup as shown in Figure V-1 was utilized in all static tests. The six hydraulic rams (see Figure V-2) were attached simultaneously to a fixed support and to a spreader beam. The spreader was in turn attached to the specimen by two one-inch diameter steel bolts passing through the extra-reinforced rear diaphragm. Two strain-gaged bolts connected the front diaphragm to the second support beam. The two support beams, W14 x 184, were held in place by two W14 x 78 steel columns. The gages were attached to the steel bolts as described in Chapter IV, Section H. Prior to each test, the hydraulic rams were connected to a portable hydraulic pump unit. The Vishay/Ellis Recorder Unit was balanced and readied for the bolt strain readings.



FIGURE V-1. LABORATORY LAYOUT FOR STATIC TEST

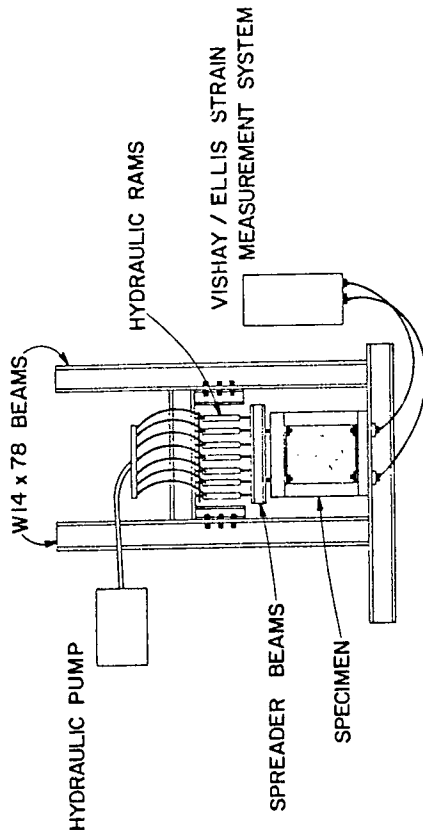


FIGURE V-2. COMPONENT IDENTIFICATION: STATIC TESTS

Typically, loading rates were approximately 50-100 pounds of total load per second or from 3000-6000 pounds of total load per minute. The Vishay/Ellis Unit automatically measured and printed on paper tape the strain at one second intervals. The results from the paper tapes were converted from strain to load; both strain and load data were kept as permanent records to accompany the photographs taken prior, during, and after each test. As a general rule, a static test was considered complete only when the load had dropped to a value of 3000 pounds or less.

In Static Test No. 4, each gaged bolt was monitored separately to determine the degree of symmetry of loading. The author discovered as the concrete specimen was loaded that either of the two bolts might carry as little as 30% or as high as 70% of the total force on the bolts. The variance between the two bolt forces was greater at small loads than at, or near, the peak load. No further tests were made with separate bolt force readings. Further, in Test No. 5 and Test No. 6, the failure crack width was measured at regular intervals of time and for each crack measurement a load reading was taken. The crack width was measured simultaneously on each side of the specimen at the neutral axis.

A sixteen-millimeter movie was made of Static Test No. 7 which shows the typical static test procedure including details of equipment operation, crack measurement, and strain recording.

### C. Dynamic Testing of Connections

Connections were specially prepared as described in Chapter III for dynamic testing purposes. These connections, seventeen in all, were tested in a custom-designed dynamic test facility to be described herein. This facility consists of the following components:

- (1) Structural support,
- (2) Beam-connection unit,
- (3) Guidance system,
- (4) Release mechanism,
- (5) Load cells (gaged bolts),
- (6) Oscilloscope and transducer plug-in unit, and
- (7) Camera recording system.

Design of the facility was based on Newton's Second Law, mathematically written as  $F = ma$ , or force equals mass times acceleration. A 5-foot horizontal beam was attached with 2 strain-gaged bolts directly to the concrete specimen. Once attached, these two items made up the beam connection unit. The unit was dropped from a height between 6 and 50 inches in such a way that each end of the beam impacted on a steel column. The connection tended to continue its downward movement and thus to separate from the beam. A tensile force was, therefore, created in the bolts holding the concrete specimen which, when it reached a critical value, failed the connection.

The basic structural elements of the test frame were two W14 x 78 columns, 20-foot tall, spaced 6-feet apart, center-to-center. Each of these columns shared a common base plate and lended lateral support to adjacent W14 x 30 columns. They were capped with a 2-inch thick bearing plate which served as a landing pad for the beam-connection unit. This unit fit between the flanges of the two W14 x 78 columns and was supported temporarily above the W14 x 30's (see Figure V-3).

Two 1-inch diameter, vertical steel bars served as guides for the free-fall of the unit. These steel bars were attached to the W14 x 78 columns and a truss work mounted on the beam connection unit incorporated two 1.24-inch I.D. steel pipes which would slide over the guide bars. The guidance system served primarily as a safety function; the levelness of the beam impact was controlled primarily by the release mechanism. The guidance system offered no restraint to the beam connection unit after the beam impacted the columns.

The release mechanism used in the dynamic tests was considered the most critical mechanical component in the setup. It consisted simply of a pair of pivoted 2-inch steel, equal-leg angle sections which could be "set" much like an animal trap to support the beam-connection unit at varying heights above the landing pads. The mechanism was tripped by a manually pulled rope attached to a pivoted handle to initiate free-fall of the beam and the adjoining concrete specimen.

The connection bolts were strain-gaged longitudinally (two gages per bolt) such that the average axial strain could be read from the

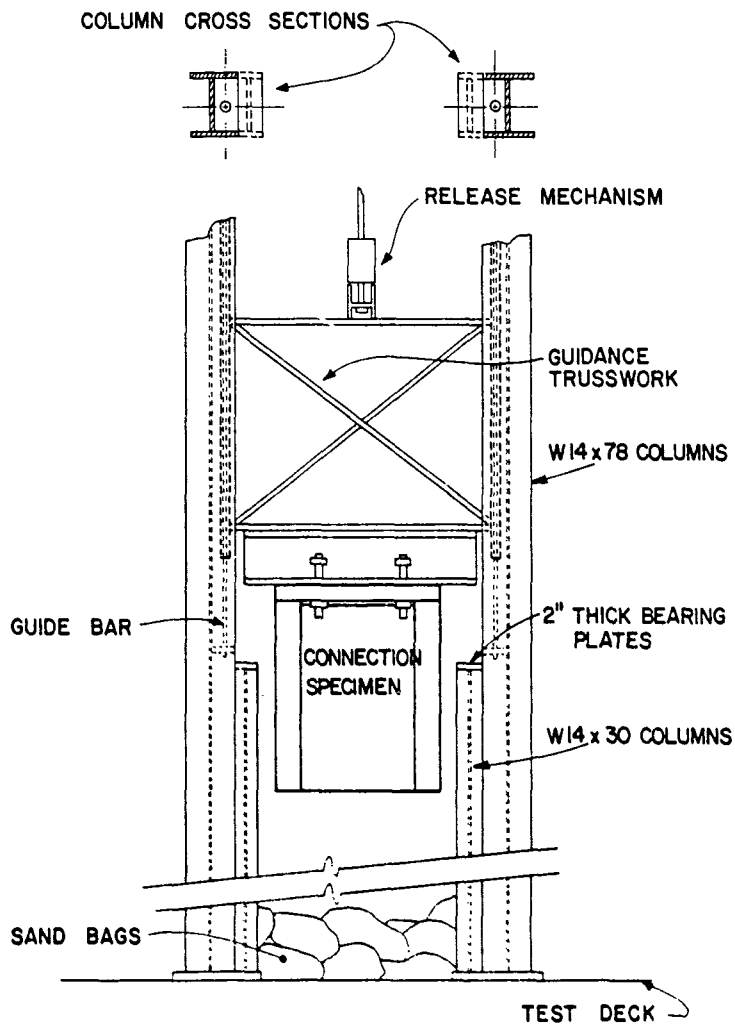


FIGURE V-3. DYNAMIC CONNECTION TEST FRAME

oscilloscope. This was accomplished by wiring the four gages on the bolts in series as one external arm of a bridge circuit and further wiring four "dummy" gages, also in series, as a second external arm of the bridge. The net output of the strain gage circuit, assuming no variation in strain on the dummy gage, was the average axial strain in the two connection bolts. The gages on the bolts were used in determining the load-time history of the specimen failure. The output from the gages was calibrated in advance (see Chapter IV, Section D) with the aid of a Timius-Olsen UEH Testing Machine.

The average strain signal was output from the oscilloscope and transducer plug-in unit in the form of a trace on the CRT. Since axial strain is simply equal to  $P/AE$  the force on the connection with respect to time could be deduced from the strain vs time trace output. An internal trigger was used to monitor the trace until initial loading commenced.

Once the specimen had been failed, records were made of the oscilloscope scale settings, peak force, and rise time: still pictures of the concrete cracks and closeups of the bent reinforcing bars were made, as necessary, to document overall damage.

#### D. Static Concrete Cylinder Tests

Three basic standard concrete tests were performed on the cylinder specimens cast during the research project: slump tests, compression tests and tensile splitting tests. A slump test according to ASTM C143-71 was made on the initial casting date; the slump was measured on this date to be 3/4-inch. Since the same mix was used throughout subsequent castings, further slump tests were not made.

All compression tests of concrete followed the specifications of ASTM C39-72. Identification numbers were placed on each specimen including the date cast and batch number. Maximum loads and compressive strengths were recorded for each test. Finally, the specimen age at testing was recorded. Figure V-4 illustrates the loading arrangement for a compression test.

All static splitting-tension tests of concrete conformed to ASTM C496-71. Identification numbers, casting dates, and batch numbers were

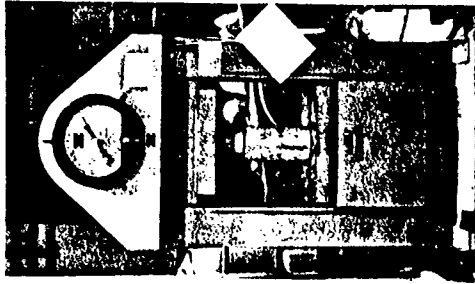
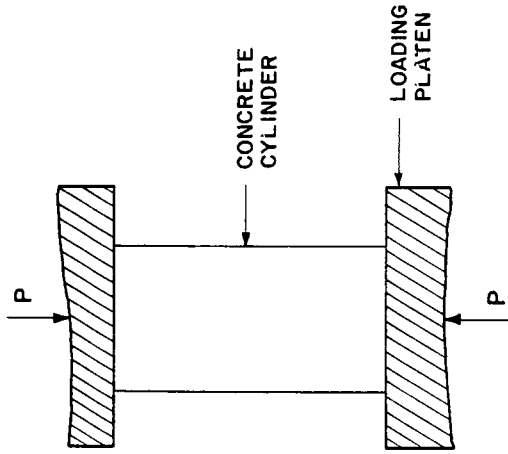


FIGURE V-4. STANDARD CONCRETE CYLINDER TESTS

recorded on each cylinder. Upon completion of each test, the maximum load and the maximum splitting stress,  $f'_{sp}$ , were recorded. Also, the age of the specimen and the percentage of coarse aggregate fractured were recorded. A typical split-cylinder test is shown in Figure IV-5.

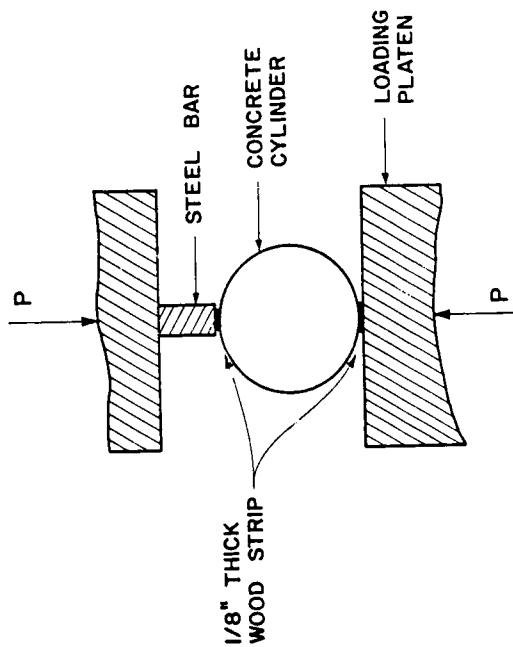
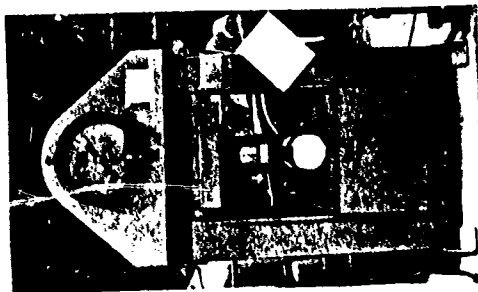


FIGURE V-5. SPLIT CYLINDER TEST



## VI EXPERIMENTAL RESULTS

### A. Static Connection Tests

Seven static connection tests were performed as summarized in Table 2. In these tests, an axial tensile force was applied to the connections at a rate in the range of from 100 to 700 pounds per second. Because of the rate of loading and because of the one-second interval between load readings on the Vishay, the maximum recorded loads and the actual maximum loads may differ slightly.

In five of the seven static tests, two local maximums are observed. The hydraulic rams providing the test load were manually operated, as nearly as possible, at a steady rate. The displacement of the rams as a function of time was monotonically increasing. In the five tests mentioned, the recorded load climbed upward to a maximum, sometimes higher, sometimes lower, than the first. The higher of these local maximums was considered to be the ultimate load. Generally, when the first maximum load was reached, the crack width at the neutral axis was approximately 1/18 inch. Static Tests No. 1 and No. 7 were the only ones in which a single load maximum was observed.

Views of the failed static specimens are shown in Figure VI-1 (A-F). Remarkable similarity was observed in crack locations as well as failure loads for the seven static tests.

For reporting purposes, the static tests specimens are divided into two categories:

- (1) Connections with deformed reinforcing bar, and
- (2) Connections with smooth reinforcing bar.

For the first group, the average initial maximum load was 20.3 kips and the average second maximum was 35.1 kips. These connections were tested at an average age of 36 days. Both of the second group specimens initially failed at 14.4 kips, and they averaged 15.1 kips for the second failure. Thirty-nine days was the average age of these specimens. The connections with 7/16-inch diameter smooth bar withstood almost 40% more load ultimately than did the connections con-

Test	Initial Maximum Load (kips)	Second Maximum Load (kips)	Age at Testing (days)	Date Cast/ Batch	f'c (ksi)	f'sp (ksi)	Comments
CONNECTIONS WITH DEFORMED REINFORCING BARS							
1	20.7	-	36	6/28/1	5.40	0.42	
2	21.5	30.2	37	6/28/2	5.29	0.47	
3	20.3	35.2	37	6/29/1	4.36	0.36	
4	18.6	33.2	37	6/29/2	4.56	0.44	
7	-	<u>41.9</u>	<u>31</u>	<u>7/13/1</u>	<u>5.56</u>	<u>0.49</u>	Test Filmed
Average	20.3	35.1	36	-	5.03	0.44	
Coefficient of Variation	6%	14%			11%	12%	
CONNECTIONS WITH SMOOTH REINFORCING BARS							
5	14.4	12.5	37	6/30/1	3.36	0.34	3/8" Rebar
6	<u>14.4</u>	17.5	40	<u>6/30/2</u>	<u>4.46</u>	<u>0.37</u>	7/16" Rebar
Average	14.4	15.1	39	-	3.91	0.36	

TABLE 2. STATIC CONNECTION TEST RESULTS

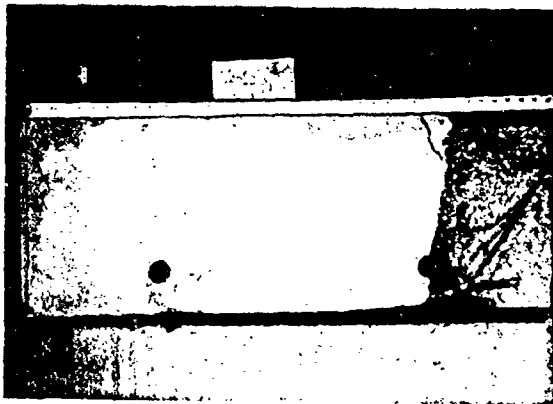


FIGURE VI-1A. STATIC CONNECTION ONE

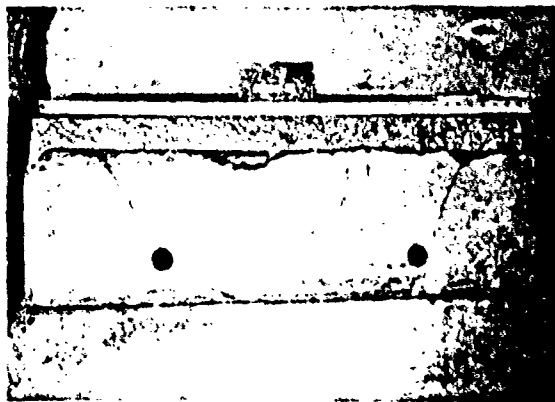


FIGURE VI-1B. STATIC CONNECTION TWO

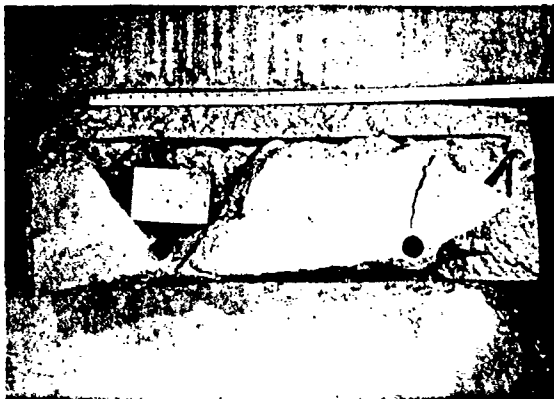


FIGURE VI-1C. STATIC CONNECTION THREE



FIGURE VI-1D. STATIC CONNECTION FOUR

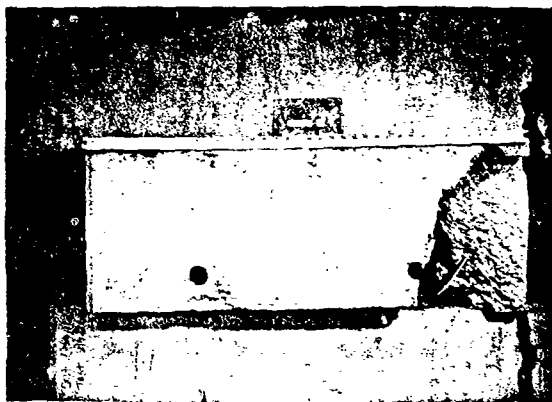


FIGURE VI-1E. STATIC CONNECTION FIVE

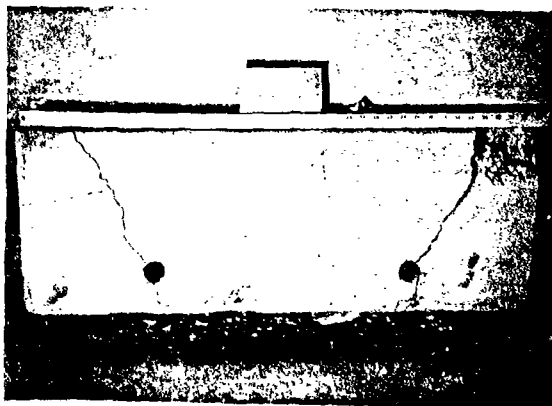


FIGURE VI-1F. STATIC CONNECTION SIX

structed with 3/8-inch diameter smooth bar. Throughout the static connection tests, No. 5 and No. 6, crack widths and corresponding loads were measured at regular intervals of time. Plots of load vs crack width are shown in Figure VI-2 (A, B).

#### B. Dynamic Connection Tests

Table 3 summarized the results of fourteen dynamic connection tests. These tests were conducted to evaluate the effects of rise-times in the range of from 5 to 30 milliseconds. To achieve this goal, drop heights and landing pads were varied throughout the test series. In spite of attempts to facilitate longer rise-times, the peak loads in all of the tests were reached in less than 4 milliseconds. A description of the landing pads used in each test is shown in Table 3.

Documentary photographs of the individual specimens after failure are included in Figure VI-3 (A-M). From these photographs one can get a good idea of the type and extent of damage withstood by the specimens. It is clear that the connection reinforcement provided a large amount of ductility. Typically, welds were broken in one or more places while, in some test cases, the reinforcing bar itself was sheared. Damage as a result of the impacts ranged from cracks of less than one inch to complete separation of the diaphragm from the remainder of the connection.

Load vs. time traces were obtained in only 8 of the 14 dynamic tests. Human error in setting the trigger mechanism, or in camera adjustments, accounted for this loss of data. Figure VI-4 is a typical photograph obtained from the oscilloscope camera. This picture, taken from Dynamic Test No. 5, has a vertical scale of 9.90 kips per square division; the horizontal scale is 2 milliseconds per square division. The individual test records were transposed to a common scale and are shown in Figure VI-5 (A-H). In Figure VI-6, the eight loads vs. time traces are shown superposed to point out similarities and differences in the load-time histories. Because of various calibration procedures, interspersed throughout the dynamic test series, the original photos recorded loads (actually strains) in each test at different vertical

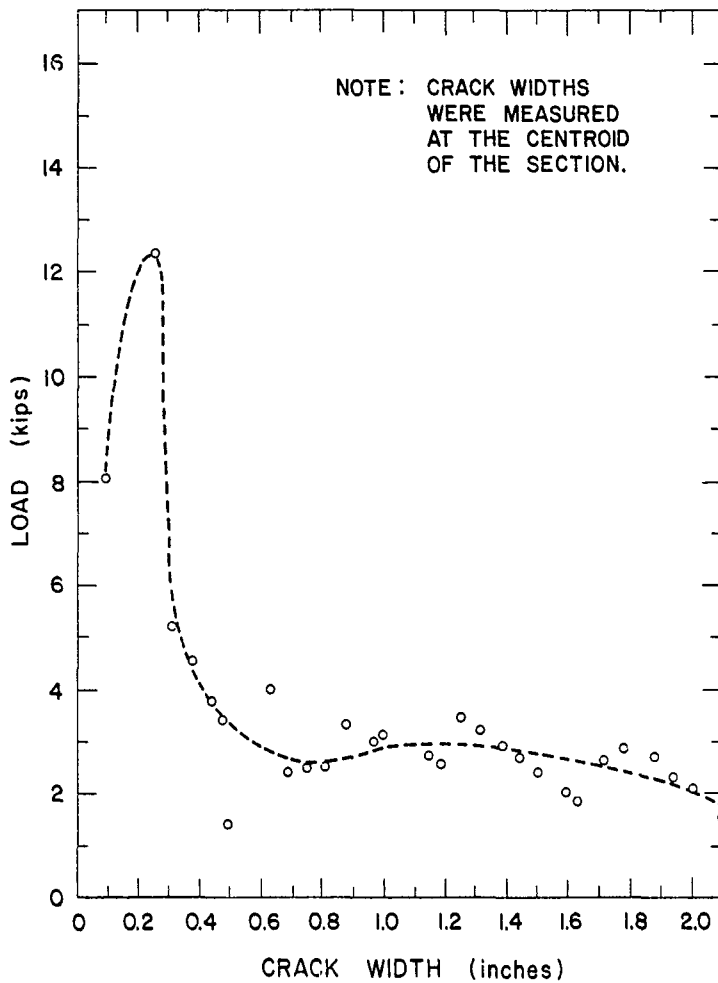


FIGURE VI-2A. LOAD VS CRACK WIDTH FOR  
STATIC TEST NO. 5

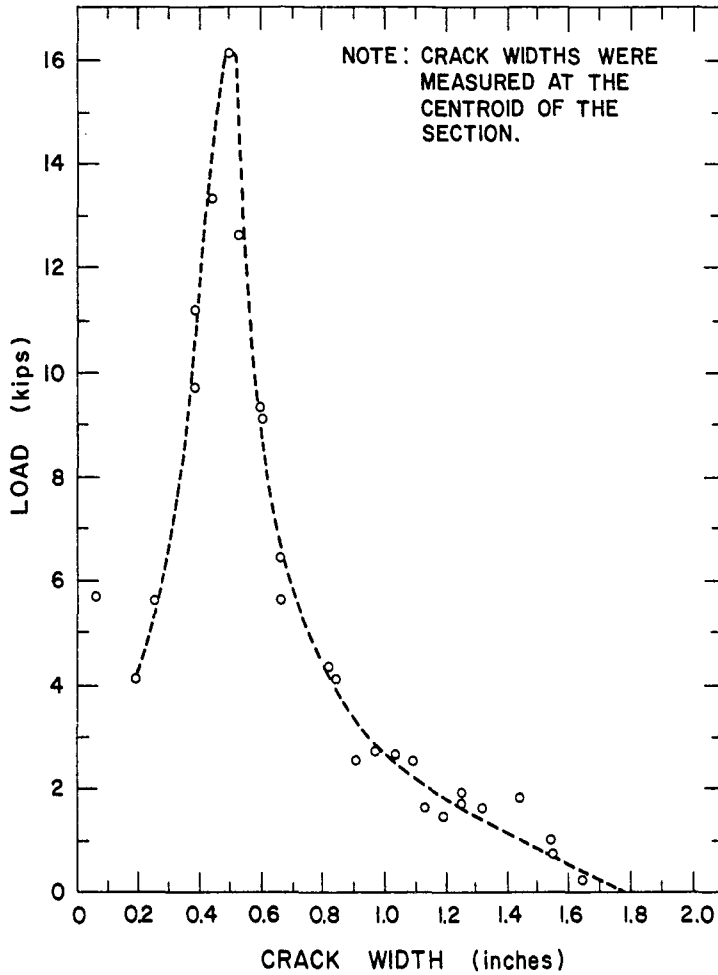


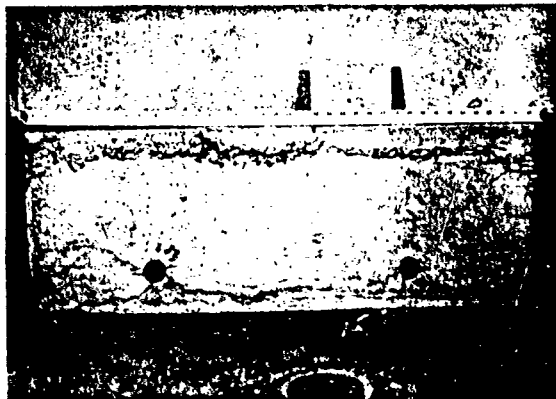
FIGURE VI-2B. LOAD VS CRACK WIDTH FOR  
STATIC TEST NO. 6

Test	Ultimate Load (kips)	Rise Time (ms)	Drop Height (in)	Residual Crack Width (in)	Age (days)	Date Cast/Batch	f'c	f'sp	Cushion
CONNECTIONS WITH DEFORMED REINFORCING BARS									
1	18.8	≥5	6.0	0.8	70	5/11/1	4.19	0.38	No Pad
2	-	-	8.4	1.4	24	6/28/2	5.29	0.47	No Pad
3	-	-	8.4	5.6	76	5/11/1	4.19	0.38	No Pad
4	22.5	-	14.4	3.0	39	6/28/1	5.40	0.42	No Pad
5	42.2	3.2	20.4	8.4	42	6/29/1	4.36	0.36	One Celotex Pad (5 sq in)
6	45.0	-	20.4	4.0	47	6/29/2	4.56	0.44	One Celotex Pad (50 sq in)
9	59.7	3.2	32.4	9.5	35	7/13/1	5.56	0.49	One Wood Pad (22 sq in)
10	-	-	32.5	5.0	35	7/13/2	4.47	0.46	Six Celotex Pads (112 sq in)
11	52.0	2.4	20.4	separation	99	5/11/2	3.80	0.44	One Celotex Pad (56 sq in)
12	37.4	3.8	20.4	6.0	99	5/11/2	3.80	0.44	Two Celotex Pads (52 sq in)
13	21.2	1.6	20.4	6.0	35	7/15/1	5.56	0.49	1" Layer of Paper Napkins (70 sq in)
14	58.8	4.0	20.8	5.0	47	7/15/2	4.47	0.46	1/4" Plywood Washers (18 sq in)
CONNECTIONS WITH SMOOTH REINFORCING BARS									
7	47.0	2.2	26.4	separation	48	6/30/1	3.36	0.34	One Celotex Pad (50 sq in)
8	44.5	2.4	26.4	3.0	48	6/30/2	4.46	0.37	One Celotex Pad (20 sq in)

TABLE 3. DYNAMIC CONNECTION TEST RESULTS



Side View

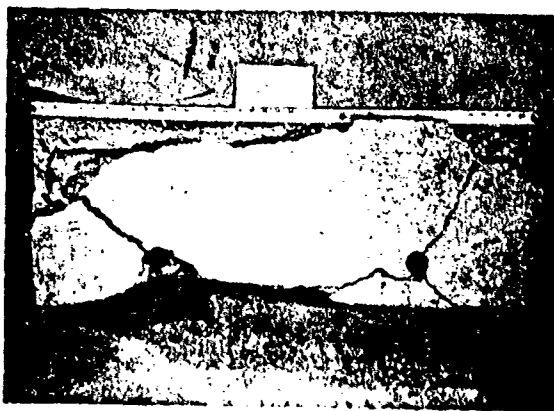


End View

FIGURE VI-3A. DYNAMIC CONNECTION ONE

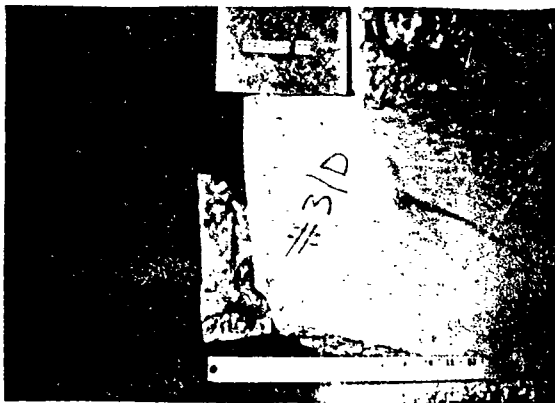


Side View

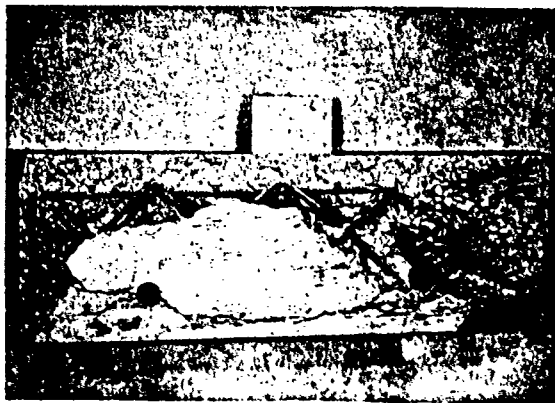


End View

FIGURE VI-38. DYNAMIC CONNECTION TWO

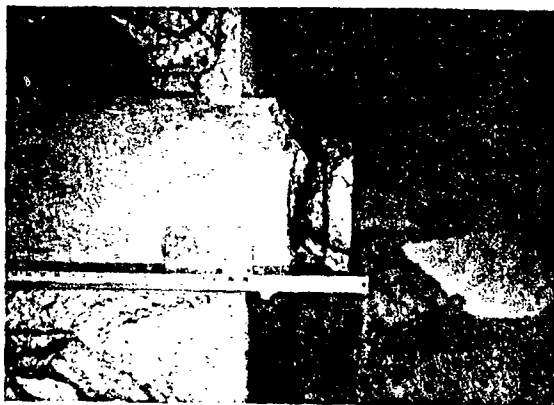


Side View

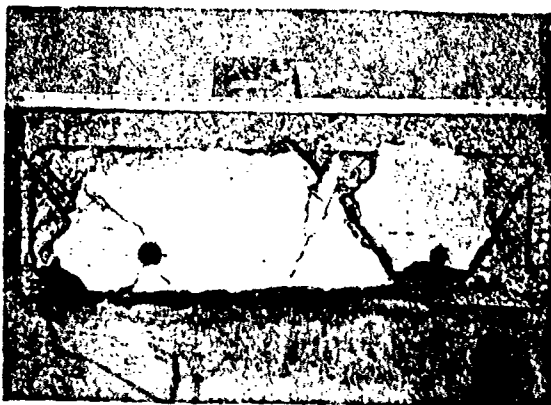


End View

FIGURE VI-3C. DYNAMIC CONNECTION THREE

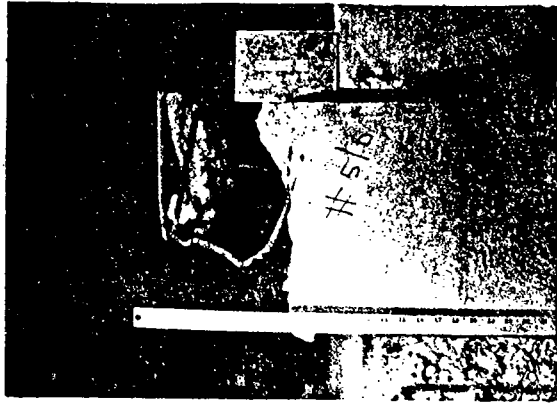


Side View

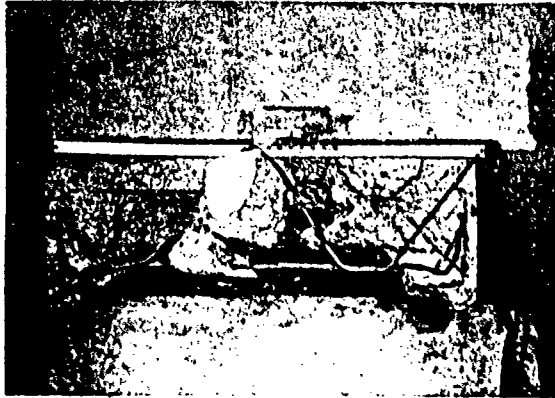


End View

FIGURE VI-30. DYNAMIC CONNECTION FOUR

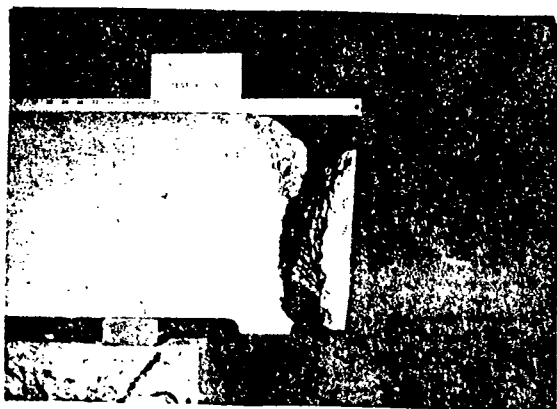


Side View



End View

FIGURE VI-3E. DYNAMIC CONNECTION FIVE

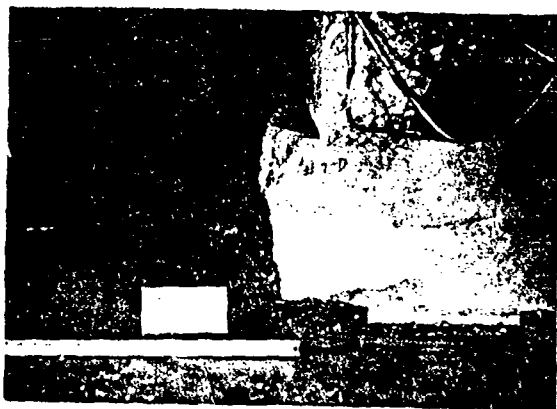


Side View

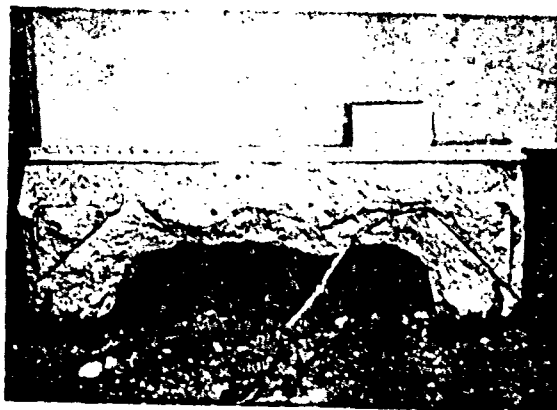


End View

FIGURE VI-3F. DYNAMIC CONNECTION SIX



Side View

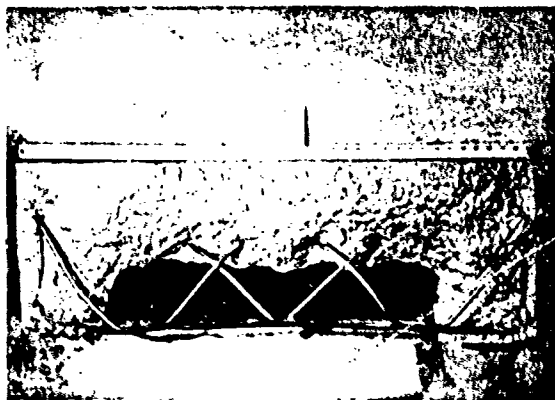


End View

FIGURE VI-3G. DYNAMIC CONNECTION SEVEN

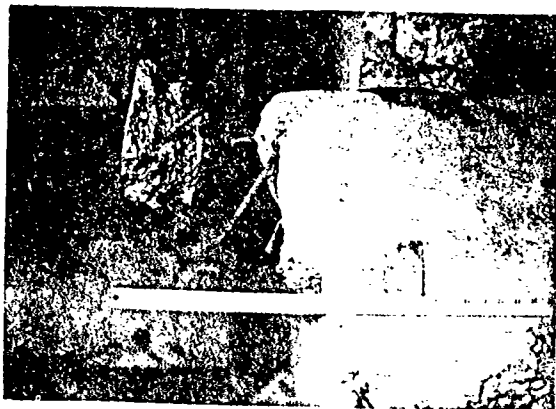


Side View

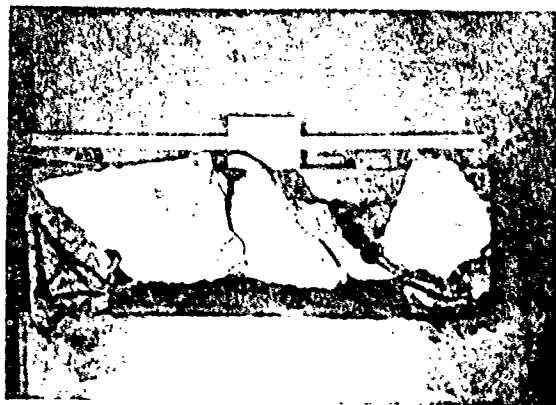


End View

FIGURE VI-3H. DYNAMIC CONNECTION EIGHT



Side View

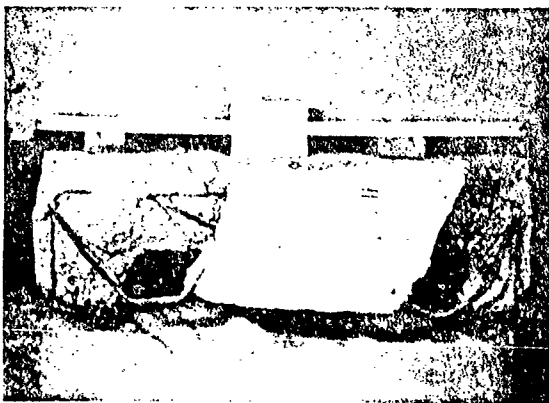


End View

FIGURE VI-31. DYNAMIC CONNECTION NINE

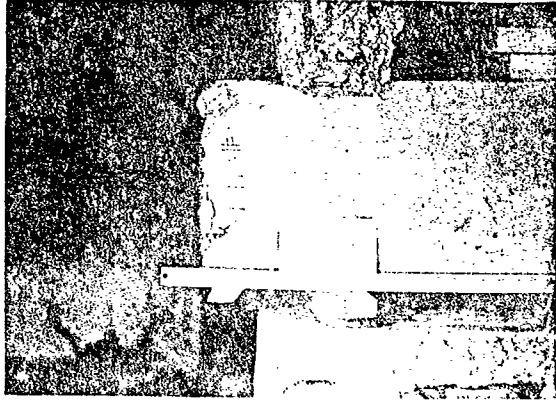


Side View

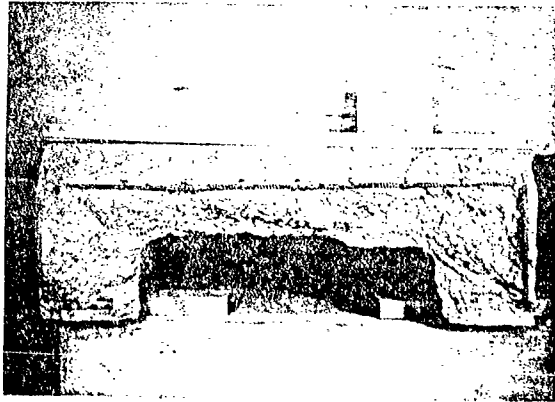


End View

FIGURE VI-3J. DYNAMIC CONNECTION TEN

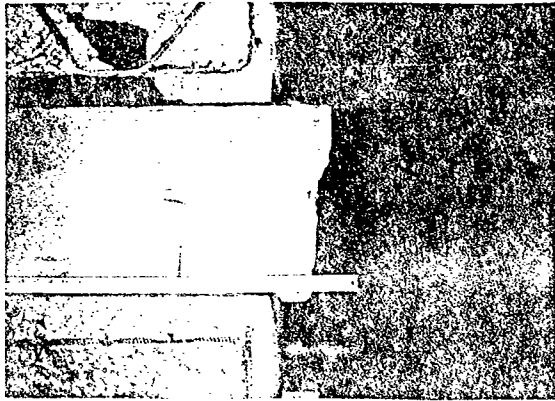


Side View

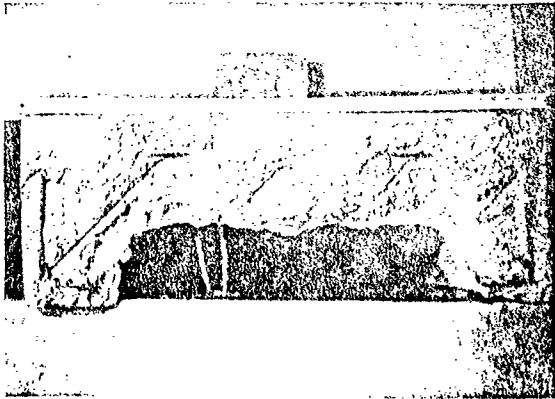


End View

FIGURE VI-3K. DYNAMIC CONNECTION ELEVEN

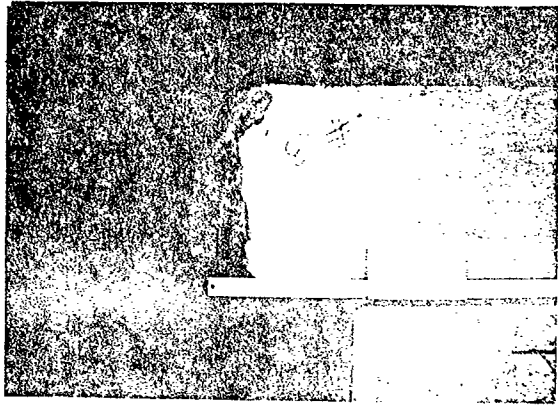


Side View

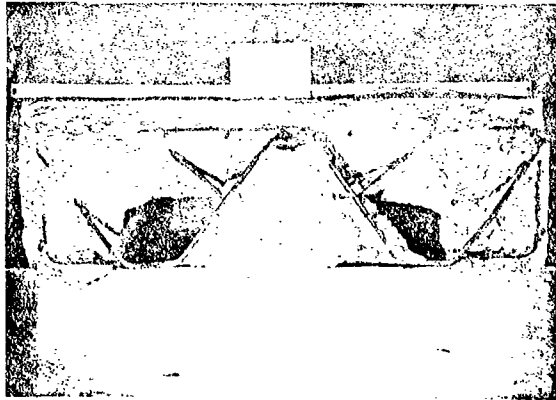


End View

FIGURE VI-3L. DYNAMIC CONNECTION TWELVE



Side View



End View

FIGURE VI-3M. DYNAMIC CONNECTION THIRTEEN

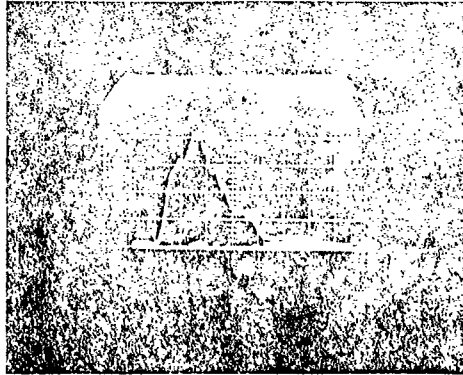


FIGURE VI-4. TYPICAL DYNAMIC TEST RECORD

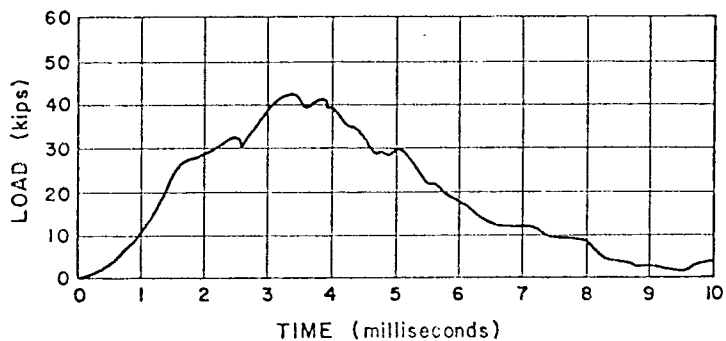


FIGURE VI-5A. DYNAMIC TEST NO. 5

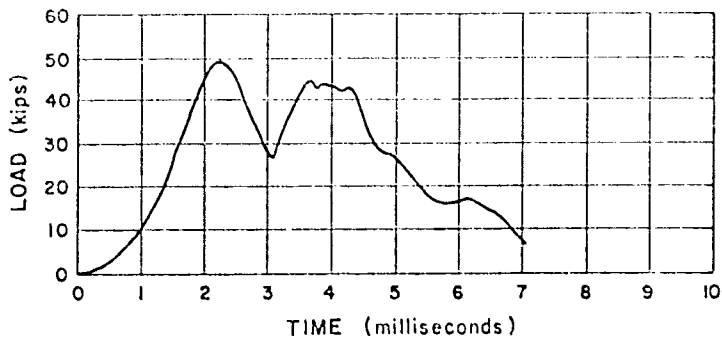


FIGURE VI-5B. DYNAMIC TEST NO. 7

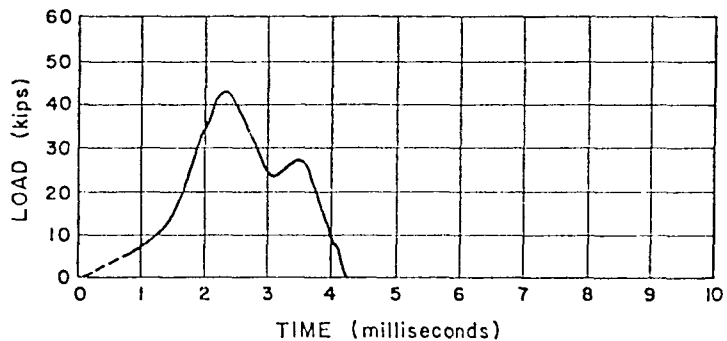


FIGURE VI-5C. DYNAMIC TEST NO. 8

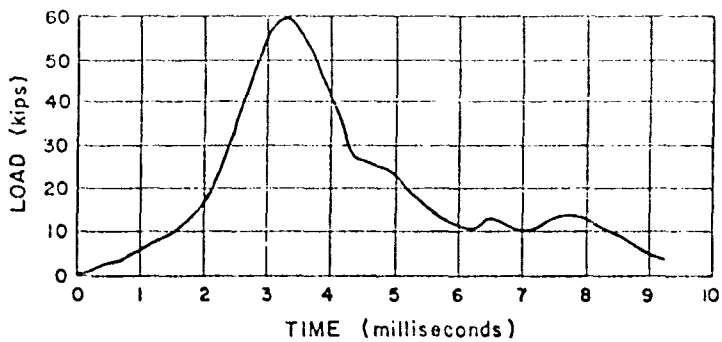


FIGURE VI-5D. DYNAMIC TEST NO. 9

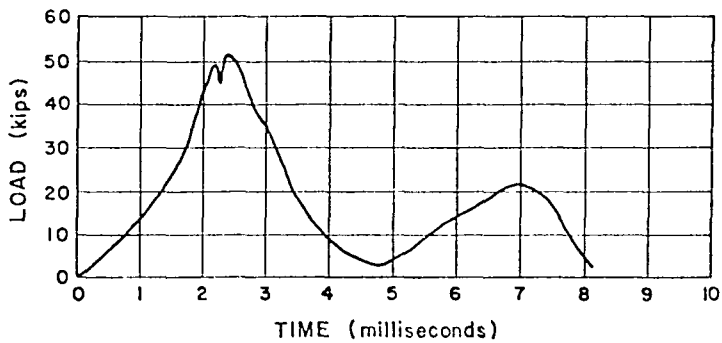


FIGURE VI-5E. DYNAMIC TEST NO. 11

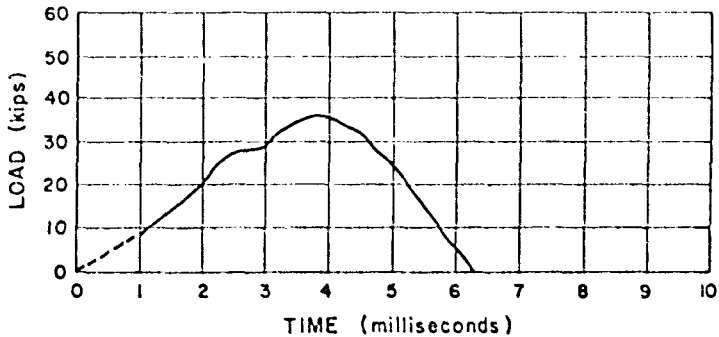


FIGURE VI-5F. DYNAMIC TEST NO. 12

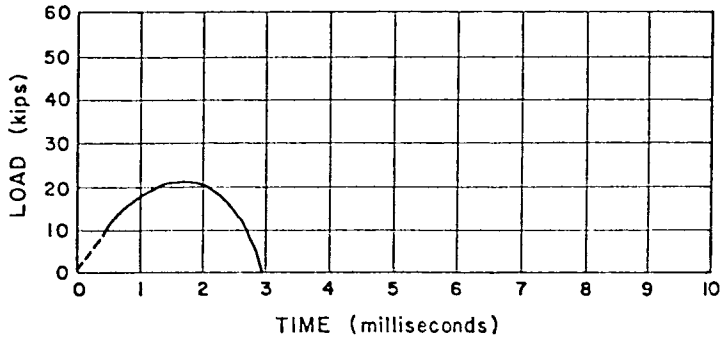


FIGURE VI-5G. DYNAMIC TEST NO. 13

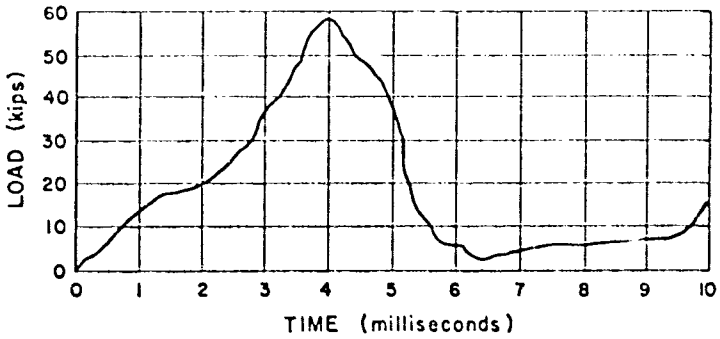
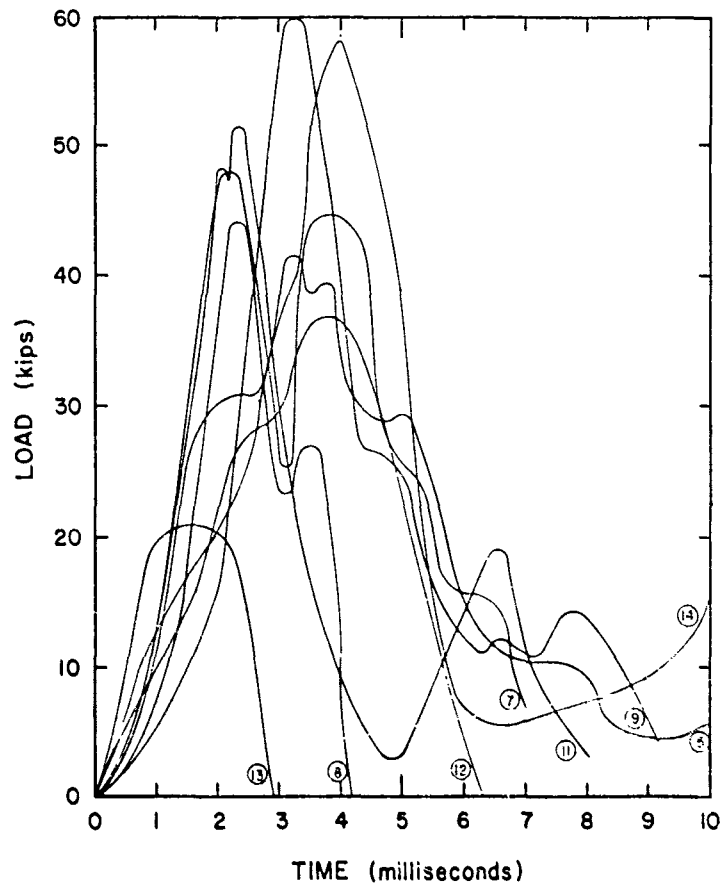


FIGURE VI-5H. DYNAMIC TEST NO. 14



⑦ - DENOTES DYNAMIC TEST NUMBER

FIGURE VI-6. SUPERPOSED DYNAMIC TEST RECORDS

Date Cast	Batch	Maximum Loads Compression (kips)			Maximum Loads Split Cylinder (kips)		
		1	2	3	1	2	3
5/11/76	1	116	117	122	41	47	42
5/11/76	2	99	100	123	46	55	47
6/28/76	1	130	159	169	48.5	47	45.5
6/28/76	2	145	159	145	50	45	55
6/29/76	1	120	121	129	37.5	41	44.5
6/29/76	2	129	130	128	49	53.5	46
6/30/76	1	72	117	96	31	30.5	55
6/30/76	2	113	127	138	40.5	43	41
7/13/76	1	158	148	166	51	59	57
7/13/76	2	130	121	128	59	47.5	51
7/15/76	1	122	119	156	70	46	54
7/15/76	2	121	123	130	41	43	47

TABLE 4. INDIVIDUAL STATIC CONCRETE CYLINDER TESTS (COMPRESSION AND SPLITTING)

Date Cast	Batch Number	Average Compressive Strength (ksi)	Average Tensile Strength (ksi)	% Aggregate Broken in Split Cylinder Test
5/11	1	4.19	0.38	75-85
5/11	2	3.80	0.44	75-85
6/28	1	5.40	0.42	75-85
6.28	2	5.29	0.47	75-85
6/29	1	4.36	0.36	75-85
6/29	2	4.56	0.44	75-85
6/30	1	3.36	0.34	75-85
6/30	2	4.46	0.37	75-85
7/13	1	5.56	0.49	75-85
7/13	2	4.47	0.46	75-85
7/15	1	4.68	0.50	75-85
<u>7/15</u>	<u>2</u>	<u>4.41</u>	<u>0.39</u>	<u>75-85</u>
Average		4.55	0.42	75-85
Coefficient of Variation	-	14%	12.6%	-

TABLE 5. BATCH CYLINDER TEST RESULTS

scales. This difference in scale prompted the author to include, rather than the original photos, scaled drawings of the traces.

Of course, when the specimens were dropped during the dynamic tests, the strain gage wires attached to the specimen bolts were moved significantly. During calibration tests, it was noted that such movement represented a strain in the order of 0.00003-inches per inch. This strain is equivalent to a load of 1.4 kips. Errors of  $\pm 5$  percent may, therefore, be present due to wire movement.

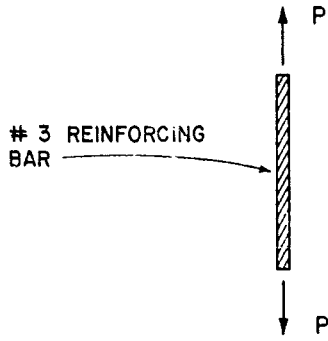
### C. Static Cylinder Test Results

Ten cylinder specimens were made per concrete batch per casting date. Three of each ten were to be statically tested in compression, three more in static splitting tension, and the remaining four in dynamic splitting tension. As mentioned in Chapter IV the ASTM split-cylinder test was chosen as a measure of the concrete tensile strength. The individual test results are shown in Table 4. It was noted that despite variations between individual test loads, the mode of failure of both compressive and tensile test specimens was of highly regular appearance. A summary of batch strengths may be found in Table 5. The average compressive strength of the concrete for the entire project was 4.62 kips per square inch; the average tensile strength was 0.43 kips per square inch.

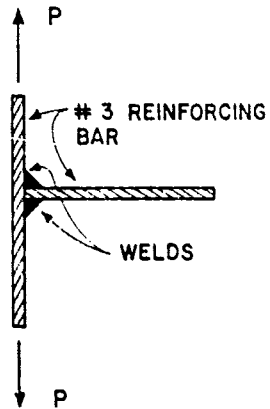
### D. Reinforcing Bar Tests

Upon receipt of each shipment of reinforcing bars, tests were conducted to ascertain the tensile strength of the steel. These tests were performed using the Tinius-Olsen UEH Testing Machine. Tensile yield strengths for the two batches of Grade 60, #3, steel reinforcement used were 76 and 79 kips per square inch. Ultimate strength for the #3 bars was measured as 86 kips per square inch. The tensile yield strength of the smooth reinforcing bar was 105 kips per square inch.

Welding of reinforcing bars for concrete is a strictly controlled process according to American Concrete Institute (ACI) design criteria. Preheating of the metal to be welded, and use of special low-hydrogen



TEST CONFIGURATION A



TEST CONFIGURATION B

FIGURE V-7. REINFORCING BAR TESTS

electrodes are two of the main requirements of reinforcing bar welds. All welds in the present program were made by student employees using E6013 electrodes; prior to welding there was no preheating of the steel.

Questions concerning connection ductility periodically recurred during construction and testing of the concrete connection specimens; such questions focused on the possible brittleness of the welded junctions of the rebars. Two simple tests were completed which served to approximate the ductility of the lab welds. Two sizes of "T"-shaped welded junctions (12 and 20 inches gage length) were constructed. Typical welding procedures were used in the construction. Similarly, two sizes of straight, non-welded reinforcing bars were tested as control specimens (see Figure VI-7).

The objective of the tests was to determine if the welding of an additional rebar affects the tensile capacity of the main rebar. For the first and second test, respectively, gage lengths of 12 and 20 inches were used. Loads and final deformations for the two tests were recorded. Deformations were measured with zero load on the specimens. Results from the two tests are given in Table 6. Permanent strain expressed as a percentage is given as the ductility.

The result of these two tests give evidence of the relatively small effect of welding on the tensile strength of the steel. In these tests, the welded specimen withstood as much or more force than the non-welded specimen. Large differences in the ductility were noted. Since this type of test indicated little difference in the tensile strength capacity of welded and non-welded reinforcing steel, further tests were not conducted.

<u>Test Number</u>	<u>Gage Length</u>	<u>Final Length</u>	<u>Yield Stress</u>	<u>Ductility</u>
1 (non-welded)	12"	14"	66.1 ksi	17%
1 (welded)	12"	12.7"	73.3 ksi	6%
2 (non-welded)	20"	23.5"	72.4 ksi	18%
2 (welded)	20"	23.25"	72.4 ksi	16%

TABLE 6. REINFORCING BAR TEST RESULTS

## VII. SUMMARY, CONCLUSIONS, AND RECOMMENDATIONS

Dynamic and static tension tests were conducted on full-scale reinforced concrete arch connections. Static tests to document material properties were performed on the reinforcing bars and on concrete cylinder specimens. The purpose of the full-scale tests was to determine the effect of the loading rate on the tensile strength of the connection.

The conclusions of previous researchers of strain-rate sensitivity of plain concrete have been somewhat contradictory, although all researchers have agreed that the strength of concrete increased with an increase loading rate. In the literature researched by this author, the largest percentage increase in strength, both in compression and in tension, was 210 percent. A brief history of strain-rate sensitivity studies of concrete has been included in Chapter II.

Seven static and fourteen dynamic connection tests were performed in this research program. In the static tests, hydraulic rams were used to apply load while strain-gaged steel bolts measured the tensile force acting on the specimen. Static ultimate loads obtained ranged from 30 to 42 kips. To carry out the dynamic test of connections, a drop tower was designed and constructed. Drop heights were varied from 6 to 32 inches; landing cushions were also varied. Resulting rise-times were between 1 and 4 milliseconds. Ultimate dynamic loads of from 19 to 60 kips were recorded. Several attempts were made to cushion the impacts and, thereby, prolong the time to failure; the cushions, however, seemed to make little difference in the rise-times obtained.

As mentioned in Chapter I, rise-times to failure of between 5 and 30 milliseconds were desired in the dynamic tests. It was hypothesized when rise-times from this range were correlated with the associated failure loads, that the relationship between rise-times and failure loads could be more clearly developed. Since the actual rise-times varied in a range of only 4 milliseconds, no such relationship could be developed.

Thirty-six static tests of concrete cylinders were also conducted. The average compressive strength of the concrete used in the project specimens was 4.55 ksi; splitting tensile strength averaged 0.42 ksi. Dynamic split cylinder tests were to have been completed on 48 specimens. Several attempts were made to construct a load cell suitable for such a test. These attempts were all unsuccessful because the load cells produced strain output signals which were too small in comparison to the noise levels within the strain measurement systems.

In 20 of the 24 connections tested, Grade 60 deformed steel reinforcement was used. Smooth, 65 ksi, steel bars were used as reinforcement in two dynamic and two static connections. The latter connection had 50 percent less static strength than the connections with deformed bars as reinforcement. In the dynamic tests, however, the smooth-bar connections sustained failure loads equal to those sustained by the deformed-bar connections.

Included in Appendix A is a brief description of previous dynamic studies on 1/3-scale arches. Presented in Appendix B are calculations of properties of both the 1/3 and full-scale, uncracked cross-section properties. Utilizing these properties, stress equations are derived which describe the maximum stress in each section as a function of the external tensile force. On the basis of these equations and the measured tensile splitting strengths of the concrete samples, static cracking loads are calculated and presented. The complexity of ultimate failure--non-linear deformations, stress intensification factors, localized homogeneity of concrete, etc., prohibited similar calculations for ultimate failure loads.

The conclusions based on this research are as follows:

- (1) Cracking failures in the static connection tests occurred as a result of combined bending and axial stresses. Theoretical cracking loads based on tensile splitting strengths were within approximately 20 percent of the corresponding experimental values.
- (2) Results of 1/3-scale static model tests were, when considering effects of scaling, in agreement with full-scale static test results.

- (3) For dynamic loadings with rise-times of from 1 to 4 milliseconds, the ultimate tensile load-carrying capacity of the connection is approximately 1.3 times as large as the static ultimate tensile load-carrying capacity. This dynamic strength factor is the ratio of the average ultimate dynamic failure load and the ultimate static failure load as measured in each case in the bolts.

Although the results of the experimental portion of this research indicated a lower value of dynamic strength factor than was initially believed, no recommendations for further testing are made. Enough confidence in the information gained in this research has been established to recommend to the USAF that further studies of the shelter connection be theoretical in nature and based on the experimental results contained herein.

## BIBLIOGRAPHY

1. Abrams, D. A., "Effects of Rate of Application of Load on the Compressive Strength of Concrete," Proceedings, American Society for Testing and Materials, Philadelphia, Volume 17, Part II, 1917, p. 364.
2. American Concrete Institute, Building Code Requirements for Reinforced Concrete (ACI 318-71), American Concrete Institute, Redford Station, Detroit, 1971.
3. Atchley, B. L., and Furr, H. L., "Strength and Energy Absorption Capabilities of Plain Concrete Under Dynamic and Static Loadings," American Concrete Institute Journal, Proceedings Volume 64, No. 11, November 1967, pp. 745-756.
4. American Society for Testing and Material, 1975 Book of ASTM Standards, American Society for Testing and Materials, 1916 Race Street, Philadelphia, 1975.
5. Biggs, J. M., Introduction to Structural Dynamics, McGraw-Hill Book Company, New York, 1964.
6. Cowell, W. L., "Dynamics Properties of Plain Portland Cement Concrete," Technical Report R-447, United States Department of the Navy, Naval Civil Engineering Laboratory, Port Hueneme, 46 pp.
7. Crist, R. A., Shear Behavior of Deep Reinforced Concrete Beams, AFWL-TR-67-61, Kirtland Air Force Base, New Mexico, October 1967.
8. DiGioia, A. M., and Crum, R. G., "Yielding at Varying Load Rates," Proceedings, American Society of Civil Engineers, Volume 88, No. EM3, June 1962, pp. 45-74.
9. Fintel, Ed., Handbook of Concrete Engineering, Van Nostrand Reinhold Company, New York, 1974.
10. Goldsmith, W., Polinka, M., and Yang, T., "Dynamic Behavior of Concrete," Experimental Mechanics, Volume 6, No. 2, February 1966, pp. 69-79.
11. Green, H., "Impact Strength of Concrete," Proceedings, The Institution of Civil Engineers (London), Volume 28, July 1969, pp. 383-396.
12. Hughes, B. P., and Gregory, R., "Concrete Subjected to High Rates of Loading in Compression," Magazine of Concrete Research, Volume 24, No. 78, March 1972, pp. 25-36.

13. Jones, P. G., and Richart, F. E., "The Effect of Testing Speed on Strength and Elastic Properties of Concrete," Proceedings, American Society of Testing and Materials, Philadelphia, Volume 36, Part II, 1936, pp. 380-391.
14. Keenan, W. A., "Dynamic Shear Strength of Reinforced Concrete Beams," Technical Report R-395, Naval Civil Engineering Lab, Port Hueneme, California, December 1965.
15. Kolsky, H., Stress Waves in Solids, Dover Publication, Inc., New York, 1963, pp. 112-116.
16. Malvern, L. E., "The Propagation of Longitudinal Waves of Plastic Deformation in a Bar of Material Exhibiting a Strain-Rate Effect," Journal of Applied Mechanics, Volume 18, No. 2, 1951, pp. 203-208.
17. Manjorine, M. J., "Influence on Rate of Strain and Temperature on Yield Stress of Mild Steel," Transactions, Journal of Applied Mechanics, American Society of Mechanical Engineers, Volume 66, No. 4, December 1944, pp. A.211-A.218.
18. Mavis, F. T., and Greaves, M. J., "Destructive Impulse Loading of Reinforced Concrete Beams," American Concrete Institute Journal, Volume 54, No. 3, September 1957, pp. 233-252.
19. Norris, C. H., et.al., Structural Design for Dynamic Loads, McGraw-Hill Book Company, New York, 1959.
20. Perry, C. C., and Lissnes, H. R., The Strain Gage Primer (Second Edition), McGraw-Hill Book Company, New York, 1962.
21. Portland Cement Association, Design and Control of Concrete Mixes (Eleventh Edition), Portland Cement Association, Skokie, Illinois, 1968.
22. Seely, F. B., and Smith J. O., Advanced Mechanics of Materials (Second Edition), John Wiley and Sons, Inc., New York, 1952.
23. Shah, S. P., and Winter, G., "Inelastic Behavior and Fracture of Concrete," Causes, Mechanisms and Control of Cracking in Concrete (Publication SP-20), American Concrete Institute, Redford Station, Detroit, 1968.
24. Smith, J. H., and Vann, W. P., "Theoretical and Experimental Investigation of Buried Concrete Structures," AFATL-TR-76-55, Air Force Armament Laboratory, Eglin Air Force Base, Florida, 1975.
25. Spooner, D. C., "Strength-Strain-Time Relationships for Concrete," Magazine of Concrete Research, Volume 23, No. 75-76.

26. Watstein, D., "Effect of Straining Rate on the Compressive Strength and Elastic Properties of Concrete," American Concrete Institute Journal, Proceedings, Volume 49, No. 8, April 1953, pp. 729-744.

## APPENDIX A. ONE-THIRD SCALE ARCH SPECIMENS

As was mentioned in Chapter I of this report, the reinforced concrete arch has been the subject of research by the Texas Tech Civil Engineering Department and the United States Air Force for the past two years. All research previous to that described in this report has been concerned with the response of buried concrete arches to dynamic loads [24]. The facilities for the experimental phase of this research included a one-third scale model of the Air Force prototype reinforced concrete arch. The factor of economy weighed most heavily in the decision to use one-third scale models in the experimental studies; the portability of the model was also considered to be of major importance. The models were also used to estimate, through the use of scaling laws, the failure strength of the full-scale prototype. Given the cylinder strength of the concrete used in constructing the arch model and the static and dynamic response of the model, one could estimate the corresponding response of a full-scale specimen. Of course the theoretical behavior of the arch, full- and one-third scale, could be calculated and compared with the experimental results. It is this comparison which was considered crucial to the refinement of a computer code designed to predict the response of buried concrete arches (see Chapter I).

The model arches, having performed their primary functions, were also used as test correlates with the full-scale connection specimens. Axial load tests performed on the connections of the arch structure became the focus of more intensive research and, thereby, the subject of this report.

During the course of the experimental one-third scale arch failure tests, the crown connection region came under close scrutiny. In both the static and the dynamic failure tests, the first indication of failure was the cracking of the reinforced concrete connection at the crown of the arch. Since this connection was the weakest element in the remaining undamaged models, only three of these tests were possible as most of the models had been damaged during the previous dynamic tests. The average tensile force required to fail the one-third scale arches was measured

to be 7.5 kips. This force was applied through a pair of prestressing cables and chucks symmetrically located at each connection bolt hole. The force in each separate cable was not monitored; only the total force in the two cables was measured.

The calculations presented in Appendix B present the theoretical relationship between the total force,  $P$ , applied through the two bolt holes, and the maximum combined bending and axial stress,  $\sigma_{pmax}$ . The quantities for  $I$  (moment of inertia),  $A$  (area), et cetera, were taken from "Theoretical and Experimental Investigation of Buried Concrete Structures" [24].

## APPENDIX B. CALCULATIONS

### Full-Scale Connection Properties

Several calculations are necessary for an analysis of the static or dynamic strength of the Air Force arch connection specimens. The following calculations were made in an attempt to estimate the failure strength of the arch connections. The reader is referred, in general, to Figure III-4c.

First, the neutral axis of the uncracked section will be located. The datum will be the underside of the "web" of the cross-section, the area of a single bar,  $A_{\text{bar}}$ , will be 0.1104 square inches. The ratio of the modulus of elasticity of steel to that of concrete is taken as 8. The computation follows:

1. Steel above datum,

$$\begin{aligned}(\Delta A)(\bar{x}_e I) (n) &= (9)(0.1104 \text{ inches}^2)(4 \text{ inches})(8) = 31.79 \text{ inches}^3 \\ n(\Delta A) &= (0.1104 \text{ inches}^2)(9)(8) = 7.95 \text{ inches}^2\end{aligned}$$

2. Steel below datum,

$$\begin{aligned}(\Delta A)(\bar{x}_e I) (n) &= (0.1104 \text{ inches}^2)(8)(5 \text{ inches})(8) = -35.33 \text{ inches}^3 \\ n(\Delta A) &= (0.1104 \text{ inches}^2)(8)(8) = 7.06 \text{ inches}^2\end{aligned}$$

3. Concrete above datum,

$$\begin{aligned}(\Delta A)(\bar{x}_e I) &= (39.38 \text{ inches})(6 \text{ inches})(3 \text{ inches}) = 709.34 \text{ inches}^3 \\ \Delta A &= (39.38 \text{ inches})(6 \text{ inches}) = 236.25 \text{ inches}^2\end{aligned}$$

4. Concrete below datum (Rectangular Sections)

$$\begin{aligned}(\Delta A)(\bar{x}_e I) &= (12 \text{ inches})(6 \text{ inches})(3 \text{ inches}) = -216 \text{ inches}^3 \\ \Delta A &= (12 \text{ inches})(6 \text{ inches}) = 72 \text{ inches}^2\end{aligned}$$

5. Concrete below datum (Draft for formwork)

$$(\Delta A)(\bar{x}e1) = (2 \text{ inches})(6 \text{ inches})(0.5)(-2 \text{ inches}) = -12 \text{ inches}^3$$

$$\Delta A = (2 \text{ inches})(6 \text{ inches})(0.5) = 6 \text{ inches}^2$$

$$\Sigma(\Delta A)(\bar{x}e1) = +477.21 \text{ inches}^3$$

$$\Sigma(\Delta A) = A = 329.66 \text{ inches}^2$$

$$\bar{X} = \frac{\Sigma(\Delta A)(\bar{x}e1)}{\Sigma(\Delta A)} = \frac{477.21}{329.66}$$

$$\bar{X} = 1.45 \text{ inches.}$$

Therefore, the neutral axis is located 1.45 inches above the datum or 4.55 inches below the top fiber of the concrete arch cross-section.

Next the moment of inertia of the uncracked section is to be found.

1. Steel above the neutral axis,

$$\Delta I = (\Delta A)(d)^2(n) = (9)(0.1104 \text{ inches}^2)(2.55 \text{ inches})^2(8)$$

$$\Delta I = 51.69 \text{ inches}^4$$

2. Steel below the neutral axis,

$$\Delta I = (\Delta A)(d)^2(n) = (8)(0.1104 \text{ inches}^2)(6.45 \text{ inches})^2(8)$$

$$\Delta I = 293.95 \text{ inches}^4$$

3. Concrete above the neutral axis,

$$\Delta I = 1/3 bh^3 = (1/3)(39.38 \text{ inches})(4.55 \text{ inches})^3$$

$$\Delta I = 1236.33 \text{ inches}^4$$

4. Concrete below the neutral axis (Flange Area)

$$\Delta I = 1/3 bh^3 = (1/3)(12 \text{ inches})(7.45 \text{ inches})^3$$

$$\Delta I = 1653.97 \text{ inches}^4$$

5. Concrete below the neutral axis (Web Area)

$$\Delta I = 1/3 bh^3 = (1/3)(27.38 \text{ inches})(1.45 \text{ inches})^3$$

$$\Delta I = 27.82 \text{ inches}^4$$

$$I = \Sigma I = 3298 \text{ inches}^4$$

#### Calculation of Static-Test Stresses (Full-Scale)

To verify the experimental tests of the static specimens, theoretical stress formulas were used to calculate the bending stress,  $\sigma$ , due to a given axial load,  $P$ ;  $P$  is applied at the bolt centerline, at a distance,  $e$ , from the neutral axis. It is assumed that the section is uncracked. The following quantities are used in the calculations:

$W = 1.43$  kips, weight of the connection.

$I = 3300$  inches<sup>4</sup>

$A = 329$  inches<sup>2</sup>

$c = 7.45$  inches

$M_p = (e)(P) = (5.45 \text{ inches})(P)$

$M_w = (e)(W) = (22.7 \text{ inches})(W)$ .

The maximum stress due to  $P$  is

$$\begin{aligned} \sigma_{\max} &= \frac{(M_p)(c)}{(I)} + \frac{(P)}{(A)} = \frac{(5.45)(P)(7.45)}{(3300)} + \frac{(P)}{329} \\ &= 0.01535(P) \end{aligned}$$

$$\sigma_{\max} = \frac{(M_w)(c)}{(I)} = \frac{(22.7)(W)(7.45)}{(3300)} = 0.0732 \text{ ksi}$$

The total stress

$$\sigma_{\max} = \sigma_w + \sigma_p = 0.01535(P) + 0.0732$$

Calculation of Static-Test Stresses (One-Third Scale)

For the one-third scale concrete arch model calculations were made to determine the theoretical maximum stress due to an axial force, P, acting through the plane of the connection bolts at a distance, e, from the neutral axis. Again the assumption is that the specimen has an uncracked section. The following quantities are used in the calculations:

$$I = 41.05 \text{ inches}^4$$

$$A = 36.25 \text{ inches}^2$$

$$c = 2.45 \text{ inches}$$

$$M_p = (e)(P) = (1.5)(P)$$

$$\sigma_{p \max} = \frac{(M_p)(c)}{(I)} + \frac{(P)}{(A)} = \frac{(1.5)(P)(2.45)}{(41.05)} + \frac{(P)}{(36.25)}$$

$$\sigma_{p \max} = 0.1171 P$$

Table 7 is a comparison of the experimental and theoretical static cracking loads as predicted from the  $f'_{sp}$ , the splitting tensile strength of the concrete used in the connections. Static Test No. 7 full-scale results were not used because no observation of a cracking load, as opposed to an ultimate load, was made. The theoretical values were obtained from the formulas derived in this appendix for both full- and one-third scale arch cross-sections:

$$P_{\text{theoretical}} = \frac{(f'_{sp} - 0.0732)}{0.01535} \text{ (ksi)}$$

for full-scale sections and

$$P_{\text{theoretical}} = 8.54 f'_{sp} \text{ (ksi)}$$

for the one-third scale section.

Test	Experimental (kips)	Theoretical (kips)	f'c (ksi)	f'sp (ksi)
FULL-SCALE				
1	20.7	22.6	5.40	0.42
2	21.5	25.9	5.29	0.47
3	20.3	18.7	4.36	0.36
4	18.6	23.9	4.56	0.44
5	14.4	17.4	3.36	0.34
6	14.4	19.3	4.46	0.37
<u>7</u>	<u>-</u>	<u>-</u>	<u>5.56</u>	<u>0.49</u>
Average	18.3	21.3	4.71	0.41
ONE-THIRD SCALE				
1	7.5	6.6 kips	8.55	0.77

TABLE 7. THEORETICAL VS. EXPERIMENTAL  
CRACKING LOADS (STATIC TESTS)